A Study of Vehicle-to-Vehicle Power Transfer Operation in V2G-Equipped Microgrid

by

Amit Kumar Tamang

A thesis
presented to the University of Waterloo
in fulfillment of the
thesis requirement for the degree of
Master of Applied Science
in

Electrical and Computer Engineering

Waterloo, Ontario, Canada, 2014

Author's Declaration

I hereby declare that I am the sole author of this thesis. This is a true copy of the thesis, including any required final revisions, as accepted by my examiners.

I understand that my thesis may be made electronically available to the public.

Abstract

Bidirectional vehicle-to-grid (V2G) system utilizes the batteries of parked electric-drive-vehicles to provide energy storage and backup services in a power system. Such services in a V2G-equipped microgrid system can be used as an enabler of enhancing the renewable energy source (RES) penetration by storing the energy during the surplus of RES supply and supplying the energy during the lack of RES supply. In this research, we aim at enhancing the storage capacity of V2G system by introducing a novel vehicle-to-vehicle power transfer operation that runs on the top of V2G services. The vehicle-to-vehicle (V2V) operation transfers the energy from the source vehicles (which are parked for relatively longer times) to the destination vehicles (which are parked for relatively shorter times). The depleted energy of the source vehicles is fulfilled by the surplus RES supply in the future. In this way, the destination vehicles are effectively charged by RES supply, thereby enhancing the storage capacity of the V2G system. We can also say that the V2V operation would become beneficial only when there is a sufficient amount of surplus RES supply in the future. We propose a decision rule to distinguish if a vehicle should be a source vehicle or a destination vehicle during the V2V operation. The decision rule is designed based on the two factors, namely the state-of-charge of vehicles battery, and the remaining time of vehicle to depart. In this research, we conduct a comprehensive study to analyze the impacts of state-of-charge and mobility pattern of vehicles on different performance metrics via simulation. The results shows that in order to achieve better performance of V2V operation, the state-of-charge of vehicles battery should be given more priority over the remaining time of vehicle to depart. The vehicle mobility pattern with unexpected departure greatly reduced the overall performance of the V2G system.

Acknowledgments

I would like to express my special appreciation and gratitude to my supervisor Professor Weihua Zhuang for her guidance, share of knowledge, encouragement, support and care. I will always be indebted to my supervisor for providing me the opportunity to pursue with my Master's degree. She was very generous on providing her invaluable advice both in research and my career. I am very thankful to her for providing me an opportunity to choose the topic of Master's research along with her invaluable suggestions. Every discussion on research with her was very encouraging and fruitful, which always broadened my knowledge. Her solid knowledge and invaluable suggestions have enriched my research. In addition to knowledge sharing, she was professional, helpful, nice, caring and always available. Professor Zhuang can be considered as a role model for the professional academic supervisor. I feel immensely privileged to work under her supervision.

I would like to extend my sincere gratitude to Professor Xuemin (Sherman) Shen and Professor Kankar Bhattacharya for serving as members of my thesis committee. I appreciate their motivation and insightful comments.

I would like to thank my colleagues at the broadband communication research (BBCR) group. The weekly group and sub-group meetings were always fruitful, which were a learning opportunity.

I am deeply indebted to my parents, my brothers Govinda and Gyan, and my sisters-in-law Kapila and Binita for their persistent motivation, support and generosity. Without their support, this thesis would not be completed.

My special thanks to my friends Jagadish and Sailesh for their help and support. I really appreciate their willingness to discuss the ideas about my research, which always helped me to enhance my understanding in the reserach. I would also like to extend my thanks to my friends Damber, Lalita and Natasha for their moral support.

Finally, I would like to thank all my friends both inside and outside of University of Waterloo for their company, help and support which made my life at Waterloo so pleasant.

Dedication

To my parents

To my brothers, Govinda and Gyan

To my sisters-in-law, Kapila and Binita

To my nephew and niece, Cyanzoe and Girwani

Contents

List of Figures

List of Tables

List of Abbreviation

AC	Altenating current
CAIFI	Customer average interruption frequency index
CHP	Combined heat and power
DC	Direct current
DER	Distributed energy resources
DG	Distributed generation
EENS	Expected energy not supplied
ESS	Energy storage system
EV	Electrical vehicle
EWMA	Exponentially weighted moving average
LC	Load controller
LOLE	Loss of load expectation
MC	Microsource controller
MGCC	Microgrid central controller
PDF	Probability density function
PEV	Plug-in electric vehicle

PHEV Plug-in hybrid electric vehicle

RES Renewable energy sources

SAIDI System average interruption duration index

SAIFI System average interruption frequency index

SOC State of charge

V2G Vehicle-to-grid

V2V Vehicle-to-vehicle

List of Symbols

$\mathbf{C^{agg}[n]}$	Aggregated charging rate of the aggregator at time-slot n
$\mathbf{C^{agg}_{max}}$	Maximum allowable aggregated charging rate of the aggregator
$\mathbf{C^{max}}$	Maximum allowable charging rate of a PHEV battery
$\mathbf{D^{agg}[n]}$	Aggregated discharging rate of the aggregator at time-slot n
$\mathbf{D^{agg}_{max}}$	Maximum allowable aggregated discharging rate of the aggregator
$\mathbf{D^{max}}$	Maximum allowable discharging rate of a PHEV battery
$\mathbf{G[n]}$	Total power supply from the utility grid at time-slot n
$\mathbf{G^{max}}$	Maximum power supply from the utility grid at a time-slot
$\mathbf{G_L[n]}$	Total power supplied to the typical microgrid load at time-slot n
$\mathbf{I}$	Total number of parking spots
$\mathbf{L[n]}$	Total typical microgrid load demand at time-slot n
$\mathbf{L_N[n]}$	Net microgrid load at time-slot n
$\mathbf{L_c[n]}$	Total load curtailment at time-slot n
$\mathbf{M_i}$	Occupancy of PHEV i
$\mathbf{N}$	Total number of time-slots
$\mathbf{P_{th}}$	Probability of unexpected departure of a PHEV at a time-slot

$\mathbf{R[n]}$	Total power supply from RES at time-slot n
$\mathbf{R_c[n]}$	Total RES curtailment at time-slot n
$\mathbf{Rv}$	Total revenue of the V2V operation
$\mathbf{SOC_i[n]}$	State-of-charge of PHEV i at time-slot n
$\mathbf{S[n]}$	Total power output of the aggregator at time-slot n
$\mathbf{T}$	Time Horizon
$\mathbf{U}$	Total cost of the V2V operation
$\mathbf{Z_i[n]}$	Random variable that indicates the unexpected departure of PHEV i at time-slot n
$\boldsymbol{\Delta}$	Duration of a time-slot
$\boldsymbol{\Gamma_{soc}}$	Average PHEV battery SOC gain
$\boldsymbol{\Omega}$	Threshold used for making a decision whether or not a PHEV discharging in the V2V operation
$\boldsymbol{\Psi_{c,n}}$	Set of charging PHEVs at time-slot n
$\boldsymbol{\Psi_{d,n}}$	Set of discharging PHEVs at time-slot n
$\boldsymbol{\alpha_\tau}$	Weight given to τ during metric $\omega_i[n]$ computation
$\boldsymbol{\alpha_{soc}}$	Weight given to SOC during metric $\omega_i[n]$ computation
$\boldsymbol{\beta}$	Self-discharging rate of a PHEV battery
$\boldsymbol{\delta_{i,min[n]}}$	Minimum charging rate demand of PHEV i at time-slot n
$\boldsymbol{\eta_c}$	Charging efficiency of a PHEV battery
$\boldsymbol{\eta_d}$	Discharging efficiency of a PHEV battery
$\boldsymbol{\gamma_B}$	Total amount of backup energy

$\boldsymbol{\gamma_S}$	Total amount of storage energy
$\boldsymbol{\gamma_{v2v}}$	Total energy from the V2V charging
$\boldsymbol{\nu_{v2v}}$	Total extra energy conversion loss due to the V2V operation
$\boldsymbol{\omega_{i[n]}}$	Metric used for making a decision whether or not PHEV i at time-slot n discharging in the V2V operation
$\boldsymbol{\overline{d_{v,i}[n]}}$	maximum energy that can be discharged from PHEV i for the V2V operation at time-slot n
$\boldsymbol{\phi_{RES}}$	Ratio of RES supply over total supply
$\boldsymbol{\tau_{i[n]}}$	Total number of time-slots remaining at time-slot n before PHEV i departs
$\boldsymbol{\tau_{max}}$	Maximum number of time-slots that a PHEV can stay parked
$\mathbf{a_i}$	Arrival time-slot of PHEV i
$\mathbf{c_i[n]}$	Total charging rate of PHEV i at time-slot n
$\mathbf{c_{G,i}[n]}$	Charging rate of PHEV i from the utility grid at time-slot n
$\mathbf{c_{V2G,i}[n]}$	Charging rate of PHEV i from RES at time-slot n
$\mathbf{c_{v,i}[n]}$	Charging rate of PHEV i due to the V2V operation at time-slot n
$\mathbf{d_i[n]}$	Total discharging rate of PHEV i at time-slot n
$\mathbf{d_{V2G,i}[n]}$	Discharging rate of PHEV i at time-slot n from RES supply
$\mathbf{d_{v,i}[n]}$	Discharging rate of PHEV i at time-slot n due to the V2V operation
$\mathbf{e}$	Capacity of a PHEV battery
$\mathbf{x_i[n]}$	Amount of charge content in PHEV i battery at time-slot n
$\mathbf{y_i}$	Total distance traveled by PHEV i before arriving at parking spot i

Chapter 1

Introduction

1.1 Microgrid and Vehicle-to-Grid System

Microgrid is a small-sized electric power system which provides electricity to a limited geographical area such as university, commercial building, hospital, industry etc. Microgrid is a self-sustained power system that can operate independently during the failure of the main grid. Hence, microgrid can be operated both in isolated mode and grid-connected mode [2] [6]. In order to be self-sustained, microgrid must contain at least one local energy resource, also known as Distributed Energy Resource (DER) [7]. DER delivers electric power through small-sized generators which reside closer to the loads. DER can be broadly classified into renewable (solar energy, wind energy) and non-renewable (diesel generator) energy resources. Renewable Energy Sources (RESs) such as solar energy and wind energy are non-dispatchable energy resources because of its uncontrollable and intermittent output. Unlike in case of diesel generator, a power system cannot control the power output of the non-dispatchable RES, according to the instantaneous changes in customers'

demand [8]. This can cause a power system failure due to the mismatch between power supply and demand. Hence, the non-dispatchable DER has a direct adverse effect on power system's quality, stability, and security. In order to minimize such adverse effects, several solutions such as spinning reserve, energy storage system (ESS), and demand side management are commonly deployed [7].

ESS can be composed of many technologies such as battery array, fly wheel, electrochemical capacitor etc. ESS can act as a storage or a supplier of energy when there is a surplus or a lack of energy in a power system (with non-dispatchable DERs) respectively. ESS plays a major role in integrating the RES into the microgrid by changing the non-dispatchable RES to a dispatchable energy resource.

Vehicle-to-grid (V2G) concept is an emerging concept which implements the battery technology for an ESS purpose. Recently, there have been many research works dedicated to this new technology [1] [9] [10] [11]. V2G system uses the batteries of electric vehicles to store and supply the electric power while the vehicles are parked. Some statistics shows that the vehicles are parked up to 96% of the time and are readily available for the V2G services [9]. This is an extremely motivating statistics towards the implementation of the V2G concept. The V2G services are *storage service* (storing surplus power of the grid) and *backup service* (supplying power back to the grid during lack of the power). A power system is typically in a need of services such as base-load power (round-the-clock service), peak power, spinning reserves (fast responding additional generation capacity) and regulation (stabilizing voltage and frequency of system during supply and demand mismatch). The V2G system can be a potentially feasible solution for both the peak load shaving service and the ancillary services (spinning reserves and regulation) [1] [9]. The peak load shav-

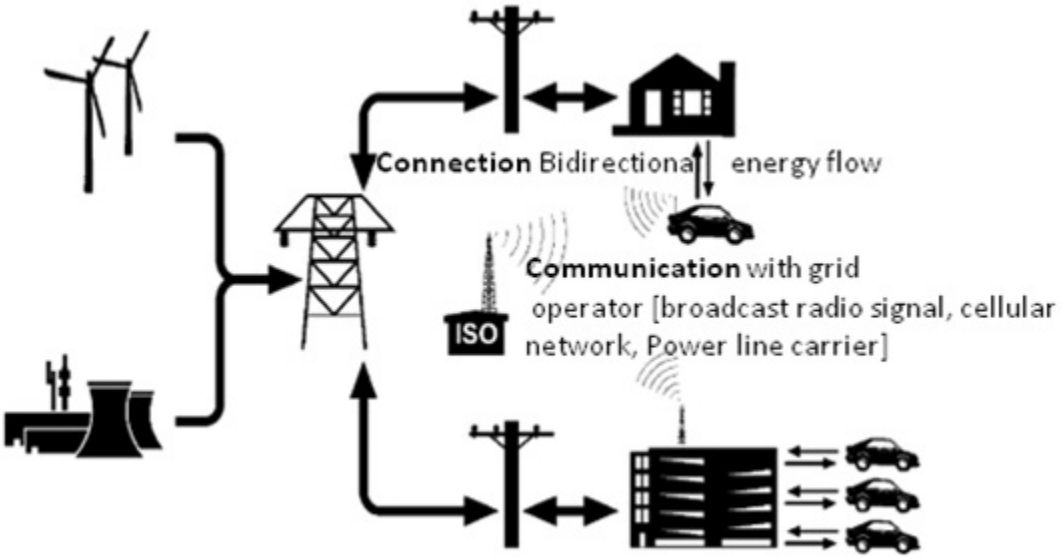

Figure 1.1: Schematic diagram to demonstrate V2G concept [1].

ing services involves a significant amount of energy transaction. In contrast, the ancillary services provide a transient capacity of supplying and absorbing the power and involves very less average amount of energy transaction. The peak load shaving service lasts for few hours while the regulation services usually last up to few minutes. Figure 1.1 demonstrates the concept of the V2G system. As shown in the figure, the electric vehicles (EV) may be plugged in a home or in a parking lot, and are equipped with an infrastructure facilitating the bidirectional energy flow with the utility grid. In order to co-ordination the power transaction, a bi-directional communication can be established with the grid operator via cellular network or power line communication.

As discussed above, in order to integrate the RES into microgrid there is a need of a resource that can act both as a generator and a storage to balance the fluctuating supply and demand. A V2G system can act as a backup, supplying power during insufficient supply of RES, or a storage, to absorb the surplus supply of RES [9]. Hence, V2G as an ESS can be viewed as a possible solution to facilitate the integration of the non-dispatchable RES

into the microgrid.

1.2 Motivation and Contribution

Literature discuss many energy storage technologies such as pumped hydro [12], flywheel [13] [14], battery [7] [14] or a combination of two or more technologies [7] [14]. The main objective of the energy storage system is to enhance the RES penetration into the microgrid, while maintaining the system stability. RES penetration can be defined as the ratio of the total energy supplied by the RES to the total energy supplied into the microgrid. Energy storage system helps an intermittent RES to become a dispatchable energy resource by smoothing out the RES's intermittent power output. ESS, thus, is an indispensable component of the microgrid, which adds flexibility and enhances the reliability of the microgrid system (by providing voltage and frequency stability of the microgrid system) [3] [8]. ESS can also provide an economic gain by storing the energy during low energy price and selling it back to the grid during high energy price. However, ESS needs higher investment [15] which increases linearly with the size of the ESS [3] [8]. As an example, ESS implemented using lead-acid batteries with size of 246 kW (power rating) and 2196 kWh (energy rating) demands initial investment cost of around $834,000 [15], and the investment cost amount is a huge. Literature also discuss the optimal sizing, which maintains the trade-off between economic and stability aspects, of the ESS in the microgrid [3] [8].

The V2G system can be a possible solution to reduce the initial investment cost on ESS. However, the V2G system provides a fluctuating size (power and energy rating) of ESS because the total number of vehicles in a parking lot keeps on changing over a period of

time. This shows that the size of the V2G-system-based ESS directly depends upon the mobility pattern of the vehicles. As an illustration, there will be more vehicles in residential area during a night-time while more vehicles will be in commercial area during a day-time. Finally, one of the key challenges in V2G system implementation is to dispatch the energy with the temporal variation of the ESS size.

Recently, there have been a number of works that discuss the integration of V2G system into the microgrid [10] [11]. Different schemes have been proposed that determine the optimal power transactions among microgrid load, microgrid supply (including RES), plug-in electric vehicles (PEV), thereby maximizing the RES penetration into the microgrid. The main challenges on designing such schemes are the uncertainty in RES generation and the dynamic size of V2G-system based ESS. In [10], three different coordinated wind-PEV energy dispatching algorithms, in the V2G context, have been proposed. The algorithms have been designed in a stochastic framework considering the uncertainties of wind power supply and the statistical PEV driving patterns. The uncertainty of wind power supply has been modeled by assuming that the wind speed follows Gaussian distribution. The arrival and departure times of PEVs are modeled by log-normal distribution. The authors of [11] proposed an optimization framework for the optimal power transaction that maximizes the RES penetration into the microgrid. The wind power generation has been modeled via scenarios with Monte Carlo simulation and scenario reduction techniques. The mobility patterns of PEVs are assumed to be deterministic.

As discussed above, the literature consider only the power transaction between PEV and grid to maximize the RES penetration. The power transaction between vehicle to vehicle has not been explored. The objective of this research is to propose a scheme that imple-

ments a novel vehicle-to-vehicle power transaction, on top of the V2G system, to enhance the RES penetration into the microgrid. The scheme also analyzes the impact of the unexpected departures of PEVs over the typical PEV mobility pattern. Figure 1.2 illustrates

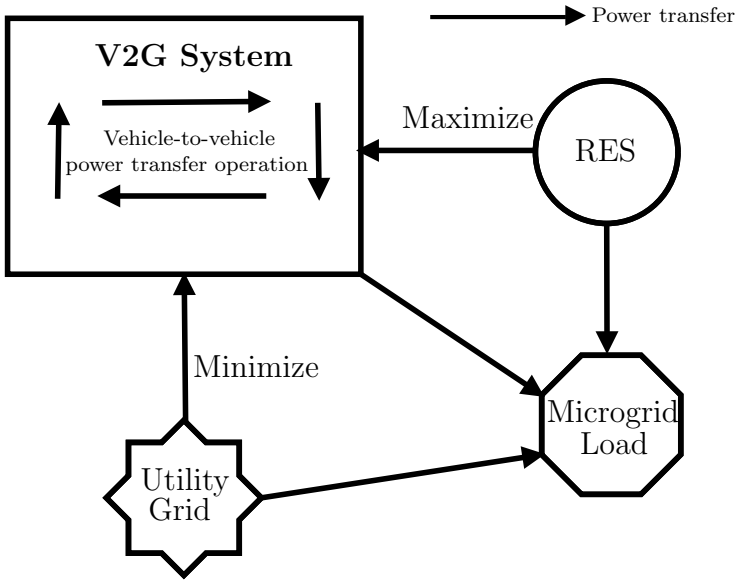

Figure 1.2: Conceptual level illustration of the vehicle-to-vehicle power transfer operation.

the concept and the role of the vehicle-to-vehicle power transaction to enhance the RES penetration. As shown in the figure, the microgrid is equipped with the V2G system and is supplied by the RES and the utility grid. The vehicle-to-vehicle power transfer operation enables the power transaction among the vehicles in addition to a typical V2G power transfer. The vehicle-to-vehicle power transactions charge the batteries of a set of destination PEVs from a set of source PEVs for a given time, thereby minimizing the total energy import form the utility grid. A source PEV is the one that departs relatively sooner and is in a need of charge in its battery, whereas a destination PEV is the one that departs relatively late and has a sufficient amount of charge in its battery. The source PEVs that supplied the energy during the vehicle-to-vehicle power transactions seek to compensate their depleted energy from the surplus RES in the future. Hence, the vehicle-to-vehicle

power transfer paradigm minimizes the total energy import from the utility grid to charge PEVs, thereby maximizing the utilization of RES (given that there is a sufficient surplus RES energy in the future). In conclusion, the RES penetration into the microgrid is further enhanced by the vehicle-to-vehicle power transaction operation in contrast to a typical V2G system.

In this thesis, we propose a scheme that determines the conditions to invoke the vehicle-to-vehicle power transfer operation in addition to the vehicle-to-grid power transfer operation. The simulation results demonstrate that the vehicle-to-vehicle power transfer operation reduces the total amount of energy import from the utility grid. It is also shown that the unexpected departure of PEVs reduces the number of vehicle-to-vehicle power transfer operation.

1.3 Outline

The reminder of the report is organized as follows. Chapter 2 provides a literature review on vehicle-to-grid (V2G) system implemented for the microgrid. Chapter 3 presents the system model of our research work. We also discuss the necessary and sufficient conditions that need to be satisfied to invoke the vehicle-to-vehicle power transfer operation, and the complete problem formulation. The performance evaluation of the scheme is presented in Chapter 4. We analyze the impact of the priority given to the state-of-charge of PEV battery and unexpected departure of PEVs on the performance of the vehicle-to-vehicle energy transaction. Finally, Chapter 5 outlines the conclusion and the future work of our work.

Chapter 2

Literature Review

In this chapter, we elaborate the concepts of the microgrid system, the energy storage system and the vehicle-to-grid (V2G) system. We also discuss the related work on the V2G system and its integration into the microgrid system.

2.1 Microgrid Power System

2.1.1 Smart Grid and Distributed Energy Resources

Smart grid concept is characterized by the notion of bi-directional flow of both electricity and information in an electric power system. The bidirectional flow of the information provides a basis for delivery of real-time information among all the components of power system (from power plants to end customers), thereby enabling the instantaneous balance of power supply and demand. Smart grid is expected to move from the traditional centralized generation approach to the distributed generation approach [16]. Distributed generation (DG) is directly implemented in the distribution system (a part of electric power system

to deliver electric energy to consumers) [17]. DG was not originally designed to connect a power generating station in traditional electric power system. The addition of DG units in the distribution system impacts the traditional electric power system into many ways. DG units help to reduce the transmission and distribution energy losses by decreasing the amount of energy drawn from the utility grid. It also enhances the system reliability by using it as a backup energy source. However, the addition of DG units can cause problems such as voltage flickering, introduction of harmonics into the system, which in turn degrades the power quality [17]. In this context, microgrid concept provides a systematic approach toward a successful integration of DG units into the distribution system, thereby acting as a key enabler for moving towards realizing the smart grid paradigm [16].

2.1.2 Microgrid Concept

Microgrid power system integrates the DG units, storage units, loads, and their control into a single subsystem as a single controllable unit. Microgrid can be operated both in a grid connected or in an isolated mode. It helps in realizing a low-emission and energy efficient system [6]. Figure 2.1 illustrates a typical architecture of a microgrid. The microgrid shown in the figure consists of three feeders (A, B, and C) with a radial feeder line configuration to transfer the power from the source to the load. The microgrid comprises of a diverse set of microsources and/or energy storage devices interconnected by a microsource controller at the right place in feeder A and B (having critical loads) to reduce line losses, support voltage, use waste heat etc. The microsources usually are low emission, low voltage sources such as renewable energy sources, fuel cells, CHP units that provide

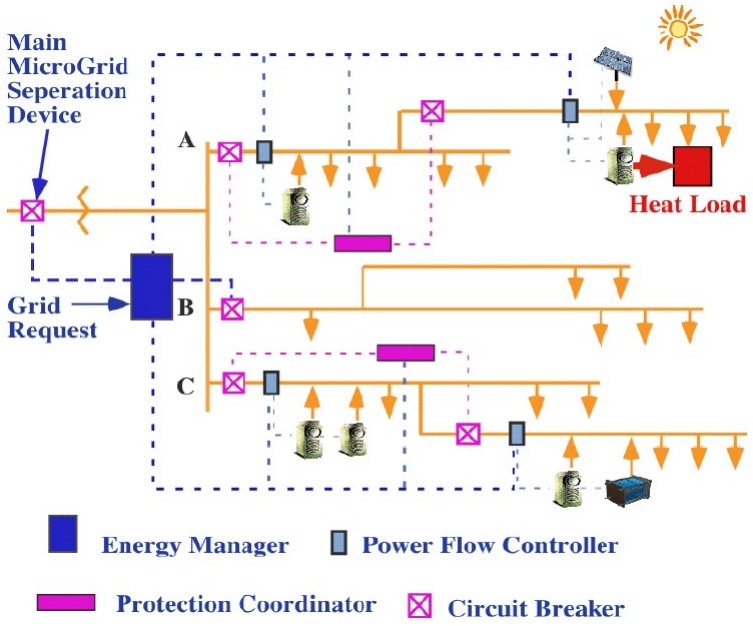

Figure 2.1: Typical microgrid architecture [2].

both heat and electricity in the vicinity. The main microgrid separation device, as shown in Figure 2.1, connects the microgrid to the utility grid. The separation device also islands the microgrid during a disturbance in either the utility grid or the microgrid itself which is helpful in maintaining the system stability. The microsource controller, which connects the microsource to the microgrid, is responsible for controlling the power and the voltage of microsource within a span of miliseconds in response to load change and disturbance. The energy manager computes the optimal energy flow within the microgrid, and between microgrid and utility grid to reduce the various costs incurred in the entire microgrid system. The power flow controllers in feeders regulate the power flow as prescribed by the energy manager. The feeder C consists of a non-critical load which can be curtailed. The protection coordinator controls the circuit breaker which isolates the faulted area within the microgrid. Hence, a microgrid consists of three different critical functions, namely microsource control, system optimization and system protection [2] [18].

The renewable energy resources generations such as solar and wind generation are intermittent in nature, hence, the output power is random and cannot be varied as required. Such renewable energy resources are considered as non-dispatchable generators. The system stability cannot be achieved with only non-dispatchable generators. Achieving high penetration of such intermittent renewable energy resources in presences of random demands from consumers is challenging in a microgrid system. The planning and operation of microgrids with consideration of such randomness are important and challenging.

2.1.3 Microgrid Planning

In microgrid planning, a decision on mixture of different kinds of distributed energy resources (such as renewable energy resources, diesel generator, battery array) and their sizing (energy and power rating) is made. The microgrid planing decision should be based on economic, environmental, and reliability aspects of the system over a span of years [19]. The key environmental aspect is the reduction of greenhouse gas emission with the use of renewable energy resources. Similarly, the economic aspect of the microgrid addresses the various costs such as fuel cost for diesel generator, electricity cost of utility grid, cost of load curtailment etc. We can find different forms of microgrid such as a utility microgrid which needs to facilitate utility grid (supply during a lack of power), a remotely located microgrid which is bound to operate in an isolated manner, and an industrial microgrid which serves critical loads [20]. Each form of microgrid adopts a different combination of distributed energy resources. As an illustration, a remotely located microgrid is impossible to be operated only with renewable energy sources because the renewable energy sources

cannot be varied according to the constantly varying microgrid load. Hence, it also needs a dispatchable energy sources such as diesel generator. This gives a combination of diesel generator and renewable energy sources for a remotely located microgrid.

The performance of microgrid planning can be assessed via various performance metrics such as system average interruption frequency index (SAIFI), system average interruption duration index (SAIDI), customer average interruption frequency index (CAIFI), expected energy not supplied (EENS), and loss of load expectation (LOLE). Hence, the microgrid planning aims at sizing a different combination of distributed energy resources to fulfill a required performance level of environmental, economic and reliability aspects.

2.1.4 Microgrid Operation

Microgrid operation determines the optimal schedule and coordination between distributed energy resources and load to minimize the overall environmental, economic and reliability cost. The intermittent renewable energy generation, random demand from customers, and random outages of components such as generation units, distribution lines introduce randomness into the microgrid. It is very challenging to obtain economic, environmental and power quality and reliability benefits in presence of such randomness. Hence, we can consider a microgrid operation as a time process in presence of uncertainties.

Literature discuss various techniques and models to deal with such randomness such as model predictive control [21], modeling randomly generated demand and renewable generation with its forecasted profile as mean and distribution of uncertainties as i.i.d. and Gaussian [22], modeling random outages of component by two-state Markov-chain with

failure and repair rate [23], Monte Carlo simulation with classification based on scenario reduction techniques and with scenario tree model [22] etc.

Hence, the microgrid operation satisfies the supply and demand balance with economic gain over a time horizon (such as a day) under the constraints such as security (voltage limit, line limit), reliability, and system component's physical constraints.

2.2 Energy Storage System

Energy storage system (ESS) stores the electrical energy using different storage technologies and deliver the electrical power when required. Energy are stored when the energy price goes down or when there is a surplus power supply. The ESS delivers back the power to loads when the price is high or when there is a lack of power supply. In addition, ESS supports the mechanisms such as load following, peak load management, and voltage and frequency stability. In microgrid, ESS mainly smooths out the intermittent output of a renewable energy source, thereby changing the renewable energy source into a dispatchable energy resource. Similarly, ESS also provides an economic gain with the energy arbitrage where the cost of energy is minimized by supplying the loads and/or selling the energy back to the utility grid during a high electricity price. Hence, ESS adds a flexibility to the power system and enhances reliability and economic gains [3] [8] of the microgrid.

2.2.1 Energy Storage Technologies

There are many storage technologies such as i) battery, which stores energy based on electrochemical reaction, ii) pumped hydro, which pumps water in a high altitude reservoir

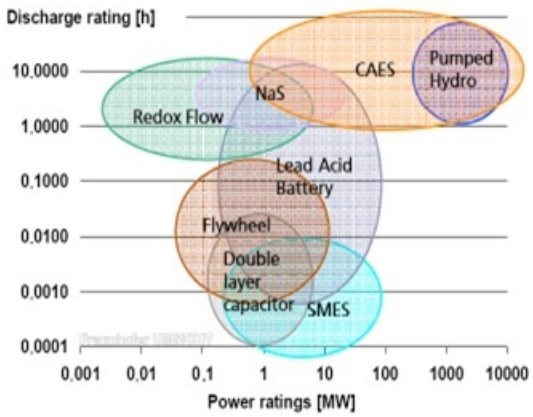

Figure 2.2: Energy storage technologies comparison [3].

using surplus power and use those pumped water again to rotate turbine and generate electricity, iii) fuel cell, which is also based on electrochemical reaction using hydrogen as the main fuel, iv) flywheel, which converts the rotational energy into the electrical energy, v) ultra-capacitor, which stores energy in an electric field and provides a surge of energy. Figure 2.2 shows a comparison of different energy storage technologies based on power rating and discharge rating [3]. The comparison assists us to select the right storage technology to satisfy our requirements. As an illustration, if we need an ESS with power rating of around 1 MW and low discharging rate, in the range of seconds, we should select ultra-capacitor storage technology. Similarly, if we need an ESS with same power rating of around 1 MW but with high discharge rating, in the range of hours, then we need to select the battery storage technology.

2.2.2 Cost of Energy Storage System in Microgrid

In microgrid, the storage technologies such as battery array, fuel cell, flywheels are widely used. Lead-acid batteries, NiCad batteries and Lithium-ion batteries are commonly used

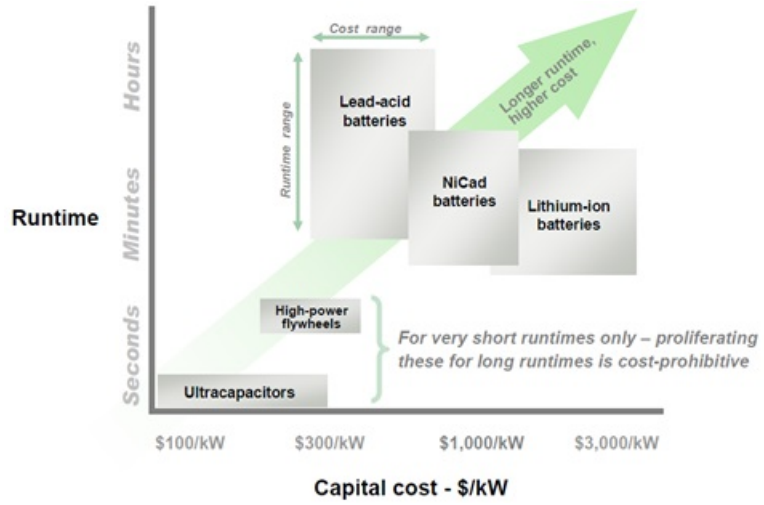

Figure 2.3: An illustration of comparison between different battery technoloies based on capital cost and runtime [4].

battery array technologies. As shown in Figure 2.3, the investment cost on battery technologies is very high in the range of \$300/kW to \$3000/kW. The authors in [15] illustrates the computation of an investment cost of around \$834000 for ESS with power rating of 246 kW and energy rating of 2196 kWh, which is a huge investment cost. ESS with such power and energy ratings is commonly required for a microgrid. Hence, there exists a trade-off between ESS investment cost and system reliability in the microgrid. There are works [8] [24] on the optimal sizing of ESS for finding the right trade-off between ESS investment cost and microgrid reliability.

Recently, there is an emerging technology called the vehicle-to-grid (V2G) system in a smart grid environment [1] [9]. The V2G system uses the vehicles that are driven by the electric energy known as the electric vehicles (EV) [25]. EVs commonly use battery (e.g., lead-acid battery) to store the electrical energy that is used in transportation. EV may be charged by the energy supplied either by utility grid and/or by RES in the microgrid. The V2G system provides a basis for energy transaction between EVs and utility

grid/microgrid. Uni-directional V2G system allows the power transfer from grid to EV, whereas bi-directional V2G system also allows the power transfer from EV to grid or vice versa. Hence, the V2G system can act as an ESS for both the utility grid and the microgrid. The main advantage of using V2G system as an ESS is that it greatly reduces the initial investment cost of ESS.

2.3 Vehicle-to-Grid System

Bidirectional vehicle-to-grid (V2G) system allows the EVs to feed the energy back to the grid while they are parked in a parking lot. The power transfer from grid to vehicle is also regarded as V2G service, to be precise uni-directional V2G [26]. V2G system mainly provides two services, namely, storage service (storing the surplus energy) and backup service (supplying energy back to the grid) [1]. In [1] different types of EVs are recognized, namely fuel cell (produce electricity on board), battery (storing energy in an electrochemical cell) and plug-in hybrid (having grid connection, allowing recharge both from grid and fuel). In this work, we consider plug-in hybrid electric vehicle (PHEV) which is relevant for the V2G system.

Based on the control method, the response time, and the duration of power dispatch, a power market can be categorized into four different types, namely baseload power, peak power, spinning reserve, and regulation. Baseload power refers to the round-the-clock service which has low per kWh price. The V2G system is not suitable for such markets. Peak power market refers to supplying power only during a high level of power consumption in a day, which normally runs few hundred hours per year and has high per kWh price.

Spinning reserves refers to an additional generating capacity which must have a fast response (in minutes) upon request. Regulation refers to stabilizing the system voltage and frequency by matching the supply and demand with response time of a minute or less. The V2G system is feasible for load shaving services (peak load) and ancillary services (spinning reserve and regulation) [1] [9].

In order to realize a V2G system, the two main elements are the charging infrastructure and the communication-and-control infrastructure. Based on voltage and current rating there are three levels of charging infrastructures. Level 1 (1.5 kVA) and level 2 (32 kVA) are slow, low power and on-board charging infrastructures. Level 3 (70 kVA) are fast, high power and off-board charging infrastructures [25]. The communication-and-control infrastructure exchanges the technical data (such as state-of-charge of battery), statistical data (such as EV's availability) and economic data (current electricity price) between the vehicles and the grid via wireless/wireline connection. Based on such information, an efficient power transaction between EVs and the grid is performed. Moreover, literature discuss the concept of an aggregator [26] [27] that integrates the capacity of many EVs to provide the V2G service. The aggreagtor provides an interface between a set of EVs and the grid such that the grid controller only needs to communicate with a single entity i.e., aggregator instead of communicating with each individual EV.

Literature provides a statistics that the vehicles (especially personal vehicles) are parked up to 96% of the time and can be available for the V2G services [1] [9] [25]. In addition, the capacity of an EV's battery has also increased over the years (recent Tesla Model S provides capacity of 85 kWh). These statistics provide a basis for the implementation of the V2G system.

2.3.1 Vehicle-to-Grid as Energy Storage System

The capacity of an ESS realized by the V2G system varies over the short duration (hours) of time. The variation in the ESS capacity is incurred due to the constantly changing total number of EVs parked in a parking lot. The authors in [28] model the V2G energy management as store-carry-and-deliver mechanism in contrast to store-and-deliver mechanism for traditional stationary battery management. Hence, the mobility of EVs has a direct impact on the capacity of the ESS. Similarly, an EV requires a certain amount of energy to be reserved in its battery for a commute purpose. This represents an energy demand from the EV itself. In [29] [30], the amount of energy reservation is determined based on the average commute energy demand of an EV. Moreover, it is also desirable to maintain the optimum level of state-of-charge in ESS such that the overall benefit of storage and backup service can be maximized. Hence, the information such as EV mobility, minimum energy demand by EV, state-of-charge of EV battery are vital in efficiently providing the V2G services. As an example, EV demand and supply in the V2G system can be modeled by an $M/M/c$ queue [31].

The arrival and departure time of an EV has been modeled by log-normal distribution with a certain mean and variance based on the statistical data [10]. In addition, a vehicle driver may take an unexpected journey and depart earlier than an expected time which adds the uncertainty in EV mobility pattern [32]. Such unexpected departure of EV makes the V2G service estimation more challenging, thereby making the V2G based energy dispatching more difficult.

Hence, the capacity of the ESS realized by V2G system is unpredictable and has highly

dynamic temporal variations. The mobility pattern of EVs greatly impacts the capacity of the ESS. The unexpected early departure should be taken into account in addition to the regular mobility pattern in order to estimate the V2G-based ESS capacity.

2.4 Related Work

V2G system can be implemented both in a large scale (e.g., utility grid) [1] [9] [26] [30] or in a small scale (e.g., microgrid) [10] [11]. There are many works which aim at developing a V2G algorithm that determines the charging and discharging rate of each EV to achieve an objective function. The objective function can be the minimization of total energy cost and/or minimization of EV owner cost [26] [27] [28] [33] [34], providing the peak shaving and ancillary services to the utility grid [30] [35], enhancing the penetration level of renewable energy resource [10] [11] [36] [37] [38] etc.

An algorithm to be used by an aggregator for the unidirectional (grid to vehicle) regulation service has been discussed in [26]. The smart charging algorithms determine a point-of-operation about which the rate of charging varies, thereby providing the regulation service. Finally, an aggregator profit maximization algorithm is formulated by considering the system load impact and the customer costs. The work provides the first logical step towards the V2G system due to the ease in implementation and has more customer acceptance. Similarly, a bidirectional V2G system is discussed in [30] addressing the benefits to both EV owners and utilities. It presents an aggregator profit maximization algorithm that provides a peak load shaving service to the utility and a low cost EVs charging. Unplanned EV departure and corresponding compensation have also been taken into consideration.

An aggregator which aggregates the distributed power of EVs to provide V2G frequency regulation services is discussed in [35]. An optimization problem formulated to minimize the overall cost arising from the battery charging after the revenue obtained by the regulation service. Finally, a dynamic programming algorithm is applied to compute the optimal charging control for each vehicle. In [28], a dynamic programming formulation is presented for minimizing the daily energy cost of vehicle owners under the time-of-use electricity pricing. Here, an exponentially weighted moving average (EWMA) algorithm is used to estimate the statistics of PHEV mobility and the non-stationary energy demand. The optimization problem for the optimal energy delivery from viewpoints of both aggregator and EV owner is formulated in [27]. The formulation presents a load shaving service taking account the randomness in vehicle mobility, time-of-use electricity pricing, and realistic battery modeling (battery degradation cost, charging and discharging constraints, self-discharging effect etc.). The non-stationary vehicle mobility is modeled by a time-dependent Markov chain. The aggregator model considers the aggregated charging and discharging power constraints of the power system.

The literature discussed above mainly aim at minimizing the EV charging cost and total energy cost, maximizing profit for an aggregator, providing services such as peak shaving to the utility grid etc. A battery system coupled with wind generators connected to a medium voltage grid is discussed in [37]. An optimal management strategy is developed to exploit the energy price arbitrage by shifting the generation along the optimization time horizon. The strategy enhances the wind generation performance by adopting it to the load demand with generation shifting policy. This promotes the integration of renewable generation into the grid. Moreover, a discrete-time model of the storage device has been

developed to address the battery dynamics such as state-of-charge, temperature, current etc. In [36], the authors explain that the renewable energy generation are intermittent and are rarely coincident with the utility load patterns. Vehicles which are typically parked more than 90% of the time can be used to store the renewable energy, and supply the stored energy during lack of supplies, thereby enhancing the utilization of renewable energy resources. The authors also discuss charge-control algorithms, overview of possible communication infrastructures such as power line communication, Zigbee, cellular network etc. V2G system which is based on a parking lot adopted in the microgrid is considered in [38]. The work proposes a coordination control strategy and also a structure in which bidirectional AC/DC and bidirectional DC/DC converters share one common DC bus. The strategy is shown to be meaningful in voltage regulation and renewable energy support. The work also presents a general microgrid model and V2G model. Similarly, a parking lot scenario for V2G system is also considered, in which an appropriate charge and discharge times throughout the day are determined such that profits to vehicle owners are maximized while satisfying the system and vehicle owners' constraints. These early works demonstrate that the research interests has sprung towards the implementation of V2G system, based on a parking lot, in a microgrid setting. The main objective in such scenarios is to enhance the utilization of renewable energy resources in microgrid satisfying the system and EV owner constraints.

In [11], the authors proposed a practical model to implement the V2G system in supporting the energy management in microgrid which includes renewable energy resources. The energy management problem is posed as a robust linear optimization problem considering the uncertainties related to renewable power sources and gridable vehicles. The work

assumes that the mobility pattern of EVs is deterministic and is already known. Wind power generation is considered as a renewable energy resource and modeled via scenario reduction technique. Finally, the robust optimization problem is constructed, based on the different wind power generation scenario, with an objective of resolving the power output/input of EVs (in garages), power output from the utility grid and the dispatchable generation units such that the total operating cost is minimized. The work focused on building a practical methodology towards the actual implementation of the V2G system and considers the uncertainty only from renewable energy resources. It is assumed that the EVs follow a deterministic mobility pattern and do not depart unexpectedly. Similarly, authors in [10] proposed a coordinated wind-PEV energy dispatching in the V2G context. Authors address the issues in a stochastic framework in which the uncertainties of wind power generation and PEV mobility pattern are discussed. The existing model of wind power generation is adopted in which the volatile nature of wind power generation is assumed to be a random variable following Gaussian distribution with time dependent mean and variance. Regarding the EV mobility, the arrival and departure time of EVs are modeled by Gaussian distribution with a certain mean time and corresponding variance. Finally, the solution aims at properly controlling the charging and discharging process of PEVs in order to improve the matching performance between power generation and consumption in the microgrid.

In conclusion, it can be said that the V2G system can contribute significantly in matching the power generation and consumption in the microgrid. Nevertheless, the scenario where curtailment of renewable energy resources is incurred can still exist. Hence, we consider a novel power transaction from vehicle to vehicle which is invoked on the top of V2G sys-

tem. By adopting the vehicle-to-vehicle (V2V) power transaction, EVs which are about to depart from the parking lot get charged from other EVs (instead of the utility grid), in addition to the charge from surplus renewable energy resources. The charge depleted, from discharging EVs, during the V2V power transfer operation will be satisfied by the surplus renewable energy resource in the future. In this way, the possible renewable energy resources curtailment incurred when only V2G system are being implemented can be minimized. Hence, the V2V power transfer operation should lead to the better utilization of renewable energy resources in the microgrid, thereby enhancing the penetration of renewable energy resources in microgrid (given that there is a sufficient surplus RES in the future).

Chapter 3

System Model and Problem Formulation

3.1 System Model

A microgrid system can operate in both grid-connected and islanded modes. We assume that the microgrid under consideration operates only in the grid-connected mode. The microgrid is also served by renewable energy sources (RES) such as solar generation and wind generation [39]. A vehicle-to-grid (V2G) system is considered as an energy storage system (ESS) for the microgrid [1]. The V2G system under consideration is bidirectional in nature. This implies that the V2G system can act both as an energy storage and as an energy supply. The architecture of microgrid system is illustrated in Figure 3.1. The microgrid is connected to the utility grid via a point of common coupling. There are a microgrid central controller (MGCC) that controls the operation of microgrid [39], and an aggregator for energy transfer with vehicles in a parking lot. The MGCC is responsible for

an optimal operation of the microgrid such that the utilization of locally generated energy (e.g., from solar and wind) is maximized. The MGCC communicates with the aggregator, the microsource controller (MC) and the load controller (LC) via a wireless (e.g., cellular)/wireline (e.g., optical fibre) communication infrastructure. The aggregator provides an interface between the set of plug-in hybrid electric vehicles (PHEVs), parked in a parking lot, and rest of the microgrid [1]. The aggregator provides the interface possibly via transformers and/or power electronics converters. The aggregator helps in energy transaction between PHEVs and the rest of the microgrid [27]. Based on the information from the aggregator, the microsource and load controllers, the MGCC determines the optimal operation point of every energy source and load, and sends corresponding control signals to the respective controllers. The controllers (MC, LC, aggregator) are assumed to have the functionality of power flow control and communication. The power flow controller in MC controls the flow of power from RES to the microgrid system. Similarly, MGCC performs the functionality of load curtailment via LC. The aggregator controls the bidirectional power flows between PHEVs and the microgrid, and among the PHEVs. The microgrid system operates over a time horizon, T. We divide the time horizon T into a number of time-slots, where each time-slot has the duration of $\Delta = T/N$, where N is the total number of time-slots. Let n denote the index of an arbitrary time-slot, $n \in \{1, 2, ..., N\}$.

3.1.1 System Supply and Demand Balance

A power system has a stringent constraint of instantaneous power supply and demand balance during its operation. The microgrid, as a power system, must maintain the said

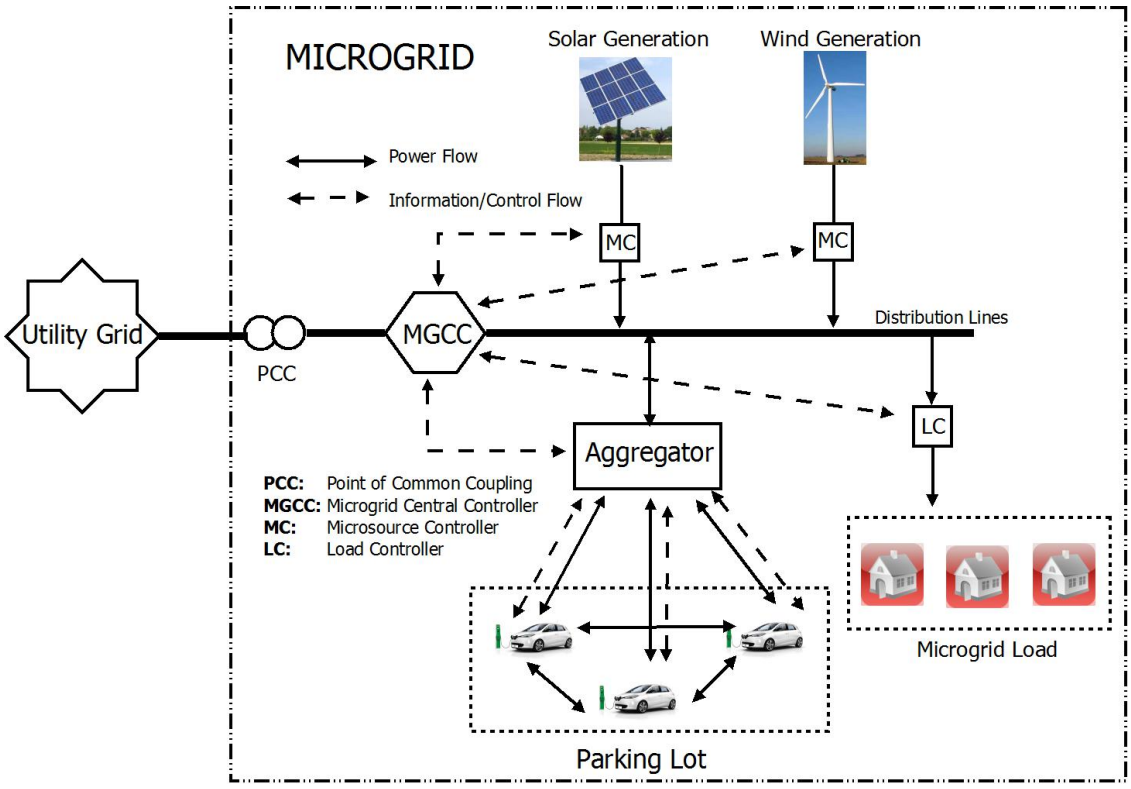

Figure 3.1: The system architecture of the microgrid.

instantaneous system supply-demand balance [10] [11]. In this research, we consider that a typical microgrid load demand is satisfied by energy supplies from the utility grid, RES and V2G service as illustrated in Figure 3.2. Here, the typical microgrid load refers to the total microgrid load demand without the charging demand from PHEVs. It also illustrates the possible load curtailment (loadshedding) or RES generation curtailment when the total supply and the total demand cannot be balanced. A supply provided by the V2G service is bidirectional in nature. The V2G service acts as a storage (backup) service when there is surplus (insufficient) RES supply, after supplied to typical microgrid loads [1]. In addition to typical microgrid loads (for example a residential load), there is a demand from the V2G system itself. A PHEV owner usually requires to have a certain amount of charge in the PHEV battery before the vehicle leaves the parking lot. The requirement imposed

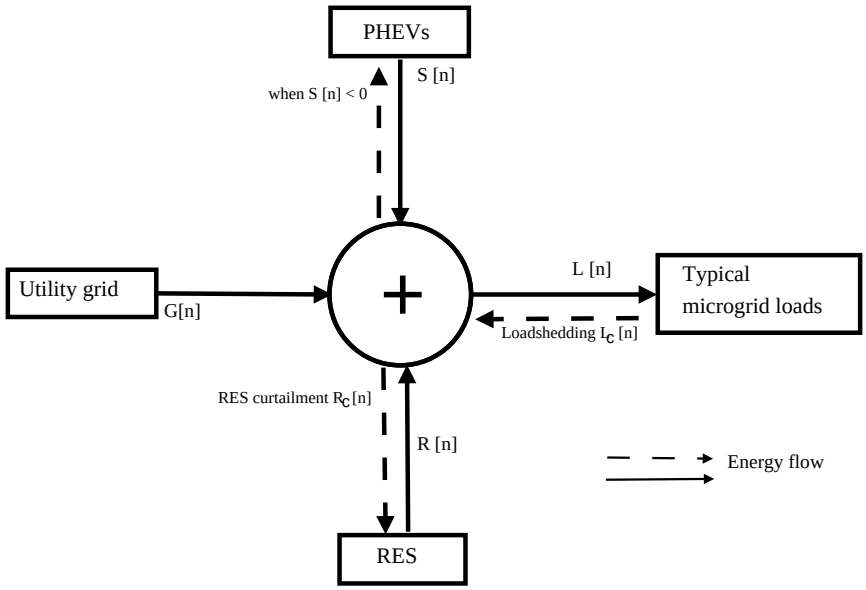

Figure 3.2: System power supply and demand balance.

by PHEV owners increases the microgrid demand, in addition to the typical microgrid loads. Such non-typical microgrid load demands will be explained in detail in the following sections.

Let $G[n]$ ($G[n] > 0$) denote the amount of power imported from the grid and $G_L[n]$ the power supplied to typical microgrid load $L[n]$, at time-slot n. Let G^{max} be the maximum allowable power imported from utility grid at any time-slot. Hence, $G[n]$ is constrained as $0 \leq G[n] \leq G^{max}$. Similarly, the total power supplied by both solar and wind RES at time-slot n is denoted as $R[n]$, which can be forecast but is inherently uncertain in nature. The uncertainty is modeled by a probability distribution function as discussed in Subsection 3.1.2. The load $L[n]$ can also be forecast with an acceptable degree of accuracy, is a typical load profile [10] [19] [40]. Let $R_c[n]$ denote the amount of RES curtailed at time-slot n ($R_c[n] \leq R[n]$), and $L_c[n]$ the amount of load curtailed at time-slot n ($L_c[n] \leq L[n]$), as illustrated in Figure 3.2. The curtailment of RES and load is

performed when the system supply and demand balance is not satisfied. Similarly, the V2G service power supplied at time-slot n is denoted as $S[n]$, which is bidirectional as discussed earlier. When $S[n] > 0$, the V2G service acts as a backup service and provides power to the microgrid load; otherwise the V2G service acts as a storage service and stores the surplus RES supply. However, when $S[n] < 0$, a set of PHEVs in the parking lot may act as load (the set of PHEVs demands more power in addition to the power supplied by RES). Such additional demand comes from the requirement to have sufficient charge level in PHEV battery before a vehicle leaves the parking lot. In summary, the system supply and demand balance equation can be written as

$$G[n] + (R[n] - R_c[n]) + S[n] = (L[n] - L_c[n]). \tag{3.1}$$

PHEV as a system load

The microgrid system needs to serve a typical microgrid load, $L[n]$. In addition to $L[n]$, a PHEV charging represents a load to the microgrid system. PHEV owners usually have a requirement of a certain range of SOC in the PHEV batteries before the vehicles leave the parking lot. Such a PHEV requirement may not be fulfilled only by the supply of RES only and additional power needs to be drawn from the utility grid. In such a situation, a PHEV acts as a system load. That is, when a PHEV charging is performed by the utility grid, the V2G system contributes to the microgrid load.

Define net microgrid load as $L_N[n] = L[n] - R[n]$, which is the microgrid load remaining to be served after RES supply. When $L_N[n] > 0$ and $S[n] > 0$, the V2G system acts as a backup and provides the power to the microgrid by discharging a set of PHEVs in the

parking lot. If $G[n] = 0$, the V2G service is able to satisfy the net microgrid load $L_N[n]$; If $G[n] > 0$, both V2G service and utility grid need to supply the net load, $L_N[n]$.

When $L_N[n] < 0$ and $S[n] < 0$, the V2G system acts as a storage and stores the energy by charging a set of PHEVs in the parking lot. This situation arises when there is a surplus power supply from RES, after serving the microgrid load $L[n]$. The situation can further be divided into two different cases: *Case 1,* V2G service acts only as a storage service when $L_N[n] < 0$ and $G[n] = 0$; *Case 2,* V2G service acts both as a storage and a load when $L_N[n] < 0$ and $G[n] > 0$.

3.1.2 RES Model

The wind generation and the solar generation are two renewable energy sources for the microgrid system, with total power generation $R[n]$ at time-slot n. Denote the power from the solar generation and the wind generation as $P_{pv}[n]$ and $P_{wt}[n]$ respectively. Hence,

$$R[n] = P_s[n] + P_w[n]. \tag{3.2}$$

Solar generation: The output of solar energy from a photo-voltaic (PV) system, $P_{pv}(t)$, depends upon PV system efficiency $\epsilon(t)$, radiation intensity $G(t)$ and temperature of solar cell [41],

$$P_{pv}(t) = \epsilon(t)G(t) \tag{3.3}$$

where $\epsilon(t)$ is a function of the solar radiation intensity (neglecting PV cell temperature) given by

$$\epsilon(t) = \begin{cases} \frac{\eta_c}{K_c} G(t), & 0 < G(t) < K_c \\ \eta_c, & G(t) \geq K_c. \end{cases} \tag{3.4}$$

In (3.4), K_c is the threshold of radiation intensity beyond which solar intensity is approximately constant equal to η_c. The intensity $G(t)$ is a function of time with both the deterministic and stochastic components which are related to geographic and atmospheric effects respectively, denoted by $G(t) = G_d(t) + G_s(t)$ [42]. The deterministic part $G_d(t)$ depends upon the time of day, season of year, latitude of location; The stochastic part $G_s(t)$ depends upon the cloud covering and weather effects, and can be modeled as a random variable at any t with a Gaussian distribution [41] [42]. Hence, the solar power generation $P_{pv}[n]$ can be modeled as a Gaussian random variable with time dependent mean and variance.

Wind generation: The output of wind turbines varies in accordance with the speed of wind at the location under consideration. Since wind speed is intermittent in nature, the output of a wind energy source at a time is a random variable. Every wind turbine has a power curve that depicts the relation between the wind turbine output and wind speed, with an example shown in Figure 3.3 [42] [5]. The output power of a wind turbine, $P_{wt}(t)$, depends upon the wind speed, v. There are three parameters associated with the wind speed: 1) V_r, rated wind speed; 2) V_{ci}, cut-in wind speed; 3) V_{co}, cut-off wind speed. For $V_{ci} \leq v \leq V_r$, the output power is a quadratic function of v; For $v < V_{ci}$ or $v > V_{co}$, there is

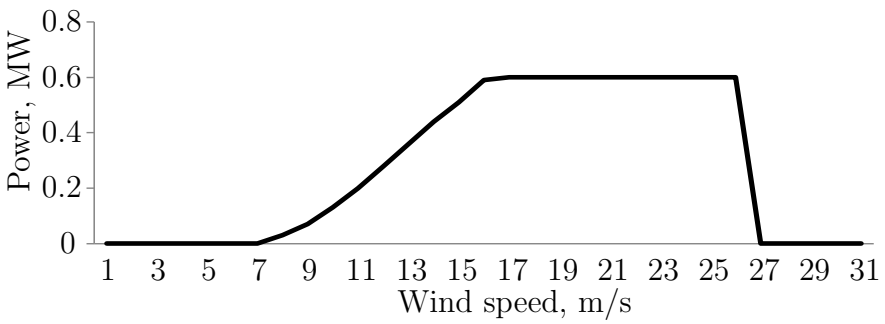

Figure 3.3: Power curve for VESTAS 600-kW wind turbine [5].

no output power [10]. The wind speed, (v), is modeled as a random variable that follows Weibull distribution [42] [43], whose probability density function (PDF) is given by

$$f(v) = \frac{k}{c}\left(\frac{v}{c}\right)^{k-1} e^{-(v/c)^k}.$$

where k and c are two parameters of Weibull distribution known as shape parameter and scale parameter respectively. The parameters are calculated from average, v_{avg}, and its standard deviation of wind speed, v_{avg} and σ as

$$k = \left(\frac{\sigma}{v_{avg}}\right)^{-1.086}$$

$$c = \frac{v_{avg}}{\Gamma(1+1/k)}.$$

The values of k and c vary according to the time of day and season of the year. Another model for the wind speed, v, is Gaussian distribution [10]. The wind generation $P_{wt}[n]$ can be computed by using the power curve for wind turbine, where the input for the power

curve is the wind speed follwing a Weibull distribution or a Gaussian distribution.

3.1.3 PHEV Battery Model

It is assumed, for simplicity, that all the PHEV batteries in the system have the same capacity and the same chemical characteristics. Denote the PHEV battery capacity by e ($e \geq 0$). We adopt the concept of state-of-charge (SOC) to resolve the amount of charge in the battery for a given time. The SOC is the available energy content in the battery normalized to its rated energy capacity. We consider a parking lot in which there are I parking spots. A parking spot is denoted by its index i, $i \in \{1, 2, ..., I\}$. Let $x_i[n]$ ($x_i[n] \geq 0$) denote the amount of charge available in PHEV i at the end of the time-slot n. We use terms "PHEV parked at parking spot i" and "PHEV i" interchangeably. Then, $x_i[n] = e \cdot SOC_i[n]$, where $SOC_i[n]$ ($SOC_i[n] > 0$) is the SOC of PHEV i at the end of time-slot n. The amount of the storage available in PHEV i at time-slot n (i.e., the maximum storage capacity of PHEV i at time-slot n) is given by $(e - x_i[n])$.

A certain amount of energy is lost during the charging/discharging process of a PHEV battery due to the energy conversion loss [44]. The energy conversion loss can be addressed by incorporating the charging/discharging efficiency of the battery into the model. Let η_c ($0 \leq \eta_c \leq 1$) and η_d ($0 \leq \eta_d \leq 1$) denote the charging and discharging efficiency of a PHEV battery respectively [33]. A PHEV battery can be charged (discharged) with a variable charging (discharging) rate, denoted by $c_i[n]$ ($d_i[n]$) for charging (discharging) during time-slot n of PHEV i battery. An illustration of the charging and discharging process of PHEV i battery during a microgrid operation is shown in Figure 3.4. It demonstrates how

the SOC in the PHEV battery is updated for each charging/discharging process. During a charging (discharging) process PHEV i's battery, the energy level is increased (decreased) by an amount of $c_i[n]\eta_c\Delta$ ($d_i[n](1/\eta_d)\Delta$) with charging (discharging) rate of $c_i[n]$ ($d_i[n]$) in time-slot n. The charging and discharging process in a battery cannot occur simultaneously at a given time [45]. In other words, we have $c_i[n].d_i[n] = 0$. Similarly, the charging/discharging rate cannot have negative values, i.e., $c_i[n] \geq 0$; $d_i[n] \geq 0$. when $c_i[n] = 0, d_i[n] = 0$, it refers to either parking spot i is empty or a PHEV plugged in at parking spot i is not charging or discharging.

The lifetime of a battery deteriorates in every charging/discharging cycle. This causes the capacity of battery (e) to decrease over each charging/discharging cycle. However, the deterioration rate of the battery is almost imperceptible over the daily cycle [46]. Hence, for the time horizon T under consideration in the system model, we do not consider the deterioration effect of the battery lifetime.

A battery exhibits an effect called "self-discharge effect". This effect causes the energy stored in a battery to be decreased over time [27]. Let β ($0 \leq \beta \leq 1$) denote the remaining fraction of the battery energy level over a time-slot or during a period of Δ due to the self-discharging effect. This implies that the maximum amount of energy available at the end of time-slot n is $\beta x_i[n-1]$, such that $x_i[n] = \beta x_i[n-1]$ when $c_i[n-1] = d_i[n-1] = 0$. Similarly, in order to prolong the lifetime of a battery, the energy level of the battery should always be maintained above a minimum threshold given by a minimum SOC, denoted by SOC_{min} [35]. Hence, $SOC_i[n] \geq SOC_{min}$.

Due to the chemical characteristics of a battery, there is a limitation over the maximum allowable charging (discharging) rate of a battery, denoted by C^{max} (D^{max}) for PHEV

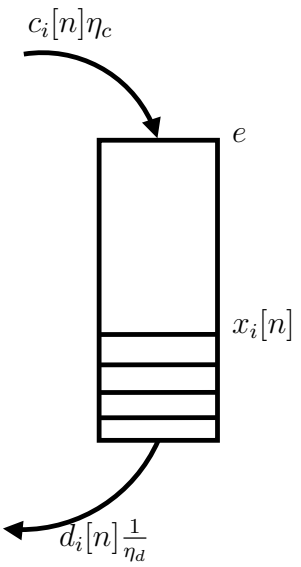

Figure 3.4: An illustration of a PHEV battery charging/discharging process at time-slot n.

i battery [27]. The charging and discharging rates are constrained as $c_i[n] \leq C^{max}$ and $d_i[n] \leq D^{max}$ respectively. Moreover, the amount of energy contained in a battery also imposes the maximum possible charging/discharging rate. The discharging rate is constrained as $(\frac{1}{\eta_d})d_i[n]\Delta \leq x_i[n]$ and the charging rate is constrained as $\eta_c c_i[n]\Delta \leq (e - x_i[n])$.

3.1.4 PHEV Mobility

The driving pattern of a PHEV owner is stochastic in nature. A deterministic model [11], a statistical model [10], and a stochastic model (Markov chain model) [27] are commonly adopted in literature for PHEV mobility. Figure 3.5a illustrates an instance of the parking lot in which a PHEV owner starts the trip from point A and ends the trip by parking the vehicle at parking spot i. The distance traveled during the trip is denoted by y_i (in km), which can be modeled by a logarithmic normal distribution, $y_i \sim LN(\mu, \sigma^2)$ [10]. For simplicity, we consider y_i to be uniformly distributed. Moreover, it is assumed that a PHEV

has a fully charged battery, i.e., $SOC = 100\%$ before it begins the trip. For example, point A can be home and PHEV battery can be fully charged over the night before it leaves home in the morning.

A PHEV consumes some energy of its battery during the trip and arrives at the parking spot i with $SOC < 100\%$. Now, PHEV i has an initial SOC, $\overline{SOC_i}$, when it arrives at parking spot i.

For a given time instance, the parking lot may have empty or occupied parking spots. Figure 3.5a illustrates that spot 2 and $i+1$ are empty, while spots 1, $i+1$ and I are occupied. Let W be the energy consumed per kilometer of the battery when a PHEV makes a trip. Then $\overline{SOC_i} = (1 - \frac{W.y_i}{e})100\%$ [10]. Hence, the initial amount of energy content in the battery of PHEV i is evaluated as $\overline{x_i} = x_i[a_i] = e \cdot \overline{SOC_i}$, where a_i is arrival time-slot of PHEV i as shown in Figure 3.5b.

We assume that an arrival process or a departure process of a PHEV occurs only at the beginning of a time-slot. The arrival process and departure process cannot occur simultaneously at the same time-slot. An arrival/departure process of a PHEV in parking spot i is illustrated in Figure 3.5b. As shown in Figure 3.5b, PHEV i arrives at the beginning of time-slot a_i with an initial SOC of $\overline{SOC_i}$ and departs at the beginning of time-slot $(a_i + \tau_i[a_i])$ or equivalently departs at the end of time-slot $(a_i + \tau_i[a_i] - 1)$, where $0 < \tau_i[a_i] < N$. We assume, for simplicity, arrival time, a_i, and departure time, $a_i + \tau_i[a_i]$, of PHEV i are uniformly distributed within a corresponding given range of time. PHEV i stays in the parking spot i for a duration of length $\tau_i[a_i]$ after its arrival at time-slot a_i. Moreover, $\tau_i[n]$ denotes the remaining number of time-slots at time-slot n for PHEV i before it leaves parking spot i. Now, let us define PHEV i occupancy, $M_i \in [a_i, a_i + \tau_i[a_i])$ to

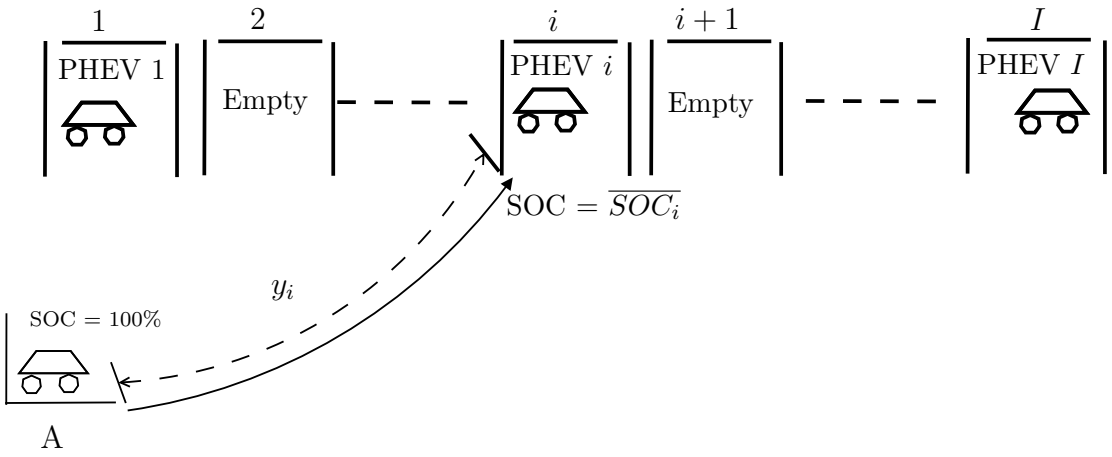

(a) PHEV arrival process in parking lot.

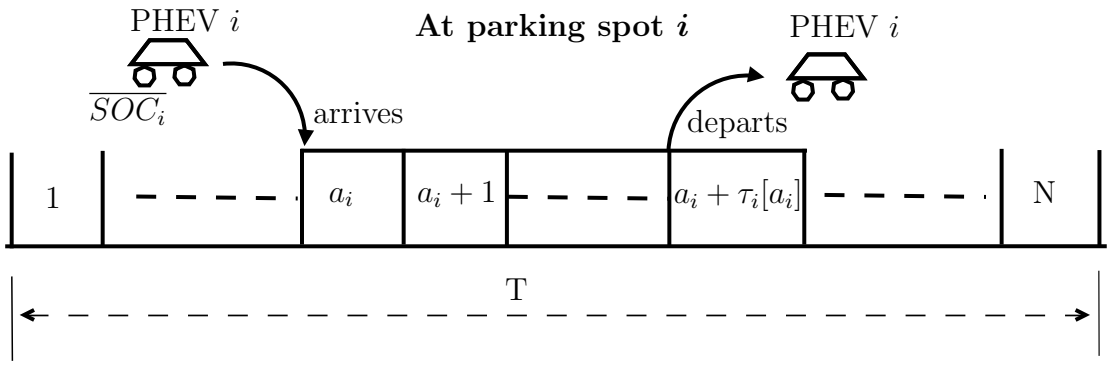

(b) PHEV arrival and departure process at parking spot i during the time horizon T.

Figure 3.5: Illustration of PHEV mobility.

be the range of time slots that PHEV i will be plugged-in where, [.) is used to represent an integer range. We assume that, for simplicity, only one PHEV can arrive and depart from parking spot i over the time horizon T. For example, it can be a scenario of a privately owned parking spot by an employee in an office. Hence, there will be maximally only one PHEV i occupancy (M_i), during the time horizon T.

We consider that a PHEV can depart earlier than an expected time. This implies a possibility that PHEV i can depart from the parking lot earlier than time-slot $a_i+\tau_i[a_i]$. In order to account for such an uncertain departure of PHEV i, let P_{th} denote the probability that PHEV i takes an unexpected early departure. Moreover, let $Z_i[n] = 0$ denote that PHEV i takes an unexpected early departure at time-slot n, and $Z_i[n] = 1$ denote that PHEV i do not take any unexpected early departure at time-slot n. We consider $Z_i[n]; \forall i, \forall n$, to be independent and identically distributed random variables, all Bernoulli distributed with success probability of $(1 - P_{th})$, then the probability mass function of $Z_i[n]$ is given as

$$f_{Z_i[n]}(z_i[n]) = \begin{cases} 1 - P_{th}, & z_i[n] = 1 \\ P_{th}, & z_i[n] = 0. \end{cases} \tag{3.5}$$

Similarly, the remaining number of time-slots, $\tau_i[n]$, is given by

$$\tau_i[n] = \begin{cases} \tau_i[a_i], & n = a_i \\ \max((\tau_i[n-1] - 1)Z_i[n], 0), & n \in M_i \text{ and } n \neq a_i \\ 0, & n \notin M_i. \end{cases} \tag{3.6}$$

PHEV batteries are not guaranteed to be fully charged before it departs. However, the PHEV i is charged as much as possible over occupancy M_i. Moreover, if a PHEV i departs only at its expected time, $a_i + \tau_i[a_i]$, the energy content will not be less than its initial energy content, $\overline{x_i}$, i.e.,

$$x_i[a_i + \tau_i[a_i]] \geq \overline{x_i}. \tag{3.7}$$

Finally, the energy content of PHEV i battery is updated according to the follwing relationship

$$x_i[n] = \max\ (\ (\beta x_i[n-1] + c_i[n]\eta_c\Delta - d_i[n](1/\eta_d)\Delta), 0\ ). \tag{3.8}$$

3.1.5 The Aggregator

The aggregator controls the charging/discharging rate of each PHEV battery in the parking lot. The control of a such charging/discharging process results in an aggregated charging/discharging rate of the aggregator as shown in Figure 3.6 [27]. The dynamics of the charging/discharging rate control of each PHEV results in either an amount of energy is drawn from (backup service) or absorbed by (storage service) the aggregator. Finally, the aggregator provides backup/storage service to support RES supply into the microgrid based on the aggregated charging/discharging process [1]. Denote $C^{agg}[n]$ as aggregated charging rate of the aggregator and $D^{agg}[n]$ as aggregated discharging rate of the aggregator, at time-slot n.

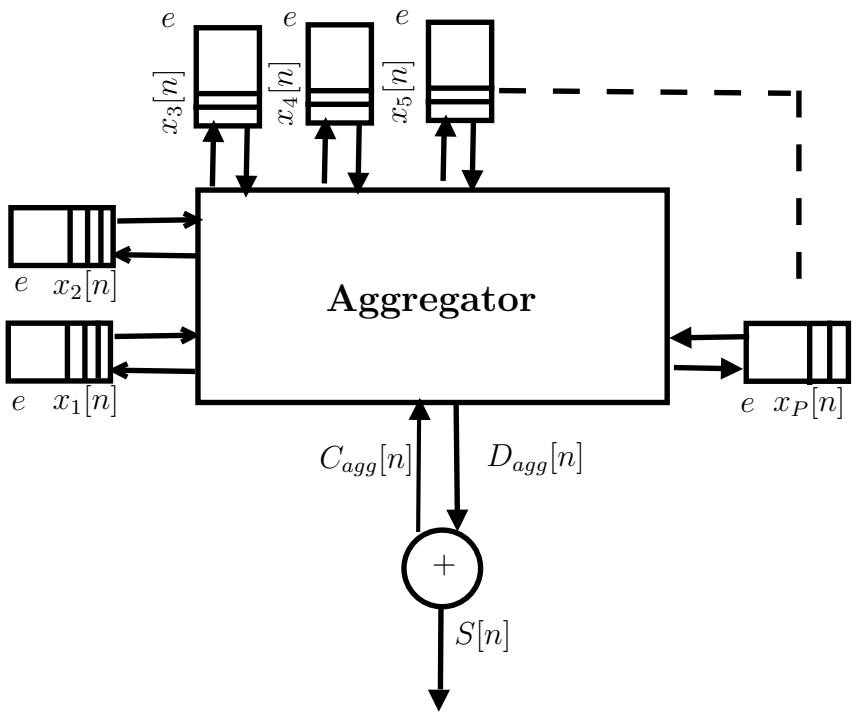

Figure 3.6: An illustration of the aggregated charging/discharging process.

The aggregator controls the energy transaction between the microgrid generation, load and a set of PHEVs parked in the parking lot. In addition, we consider a novel approach in which the aggregator performs the energy transaction among the PHEVs within the parking lot, irrespective of the other generations and load in the microgrid. Finally, charging rate $c_i[n]$ and discharging rate $d_i[n]$ of PHEV i are divided into different components as demonstrated in Figure 3.7. The PHEV charging rate consists of three different parts: i) a charging rate from the other PHEVs, $c_{v,i}[n]$, ii) a charging rate from the surplus RES generation (storage V2G service), $c_{V2G,i}[n]$, and iii) a charging rate from the utility grid, $c_{G,i}[n]$. Similarly, a PHEV discharging rate consists of two different parts: i) a discharging rate to other PHEVs, $d_{v,i}[n]$, and ii) a discharging rate to support lack of RES generation (backup V2G service), $d_{V2G,i}[n]$. Hence, the total charging rate $c_i[n] = c_{v,i}[n] + c_{V2G,i}[n] + c_{G,i}[n]$ and total discharging rate $d_i[n] = d_{v,i}[n] + d_{V2G,i}[n]$.

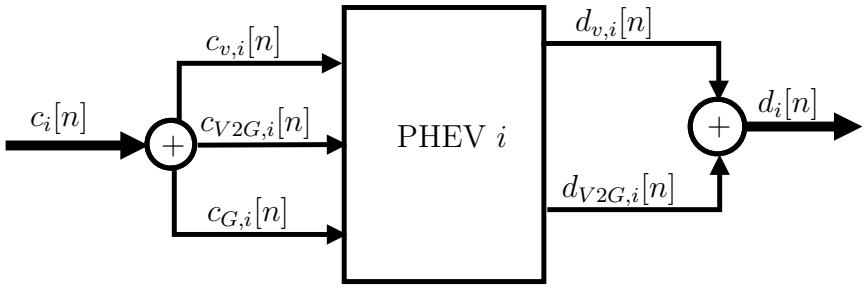

Figure 3.7: Different parts of the charging/discharing rate of a PHEV.

For a demonstration purpose, an example of the energy transaction process among the PHEVs, at time-slot n, is shown in Figure 3.8 where a set of PHEVs are in the charging mode and another set of PHEVs is in discharging mode. PHEV i (a representative of the set of discharging PHEVs) has two components of discharging rates $d_{v,i}[n]$ and $d_{V2G,i}[n]$. Similarly, PHEV j (a representative of the set of charging PHEVs) has three components of charging rates $c_{v,j}[n]$, $c_{G,j}[n]$ and $c_{V2G,j}[n]$. It should be noted that the rates $c_{v,i}[n]$ and $d_{v,i}[n]$ do not contribute to the aggregated charge and discharge rates out of the aggregator. In conclusion, the following relations can be listed.

- $D^{agg}[n] = \sum_{i=1}^{I} d_{V2G,i}[n]$;
- $C^{agg}[n] = \sum_{i=1}^{I} (c_{V2G,i}[n] + c_{G,i}[n])$;
- $S[n] = D^{agg}[n] - C^{agg}[n]$, which is referred as the net power output of the aggregator;
- The sum of charging rate $c_{v,i}[n]$ from all parking spots must be equal to the sum of discharging rate $d_{v,i}[n]$ from all the parking spots at a given time-slot:
  $\sum_{i=1}^{I} c_{v,i}[n] = \sum_{i=1}^{I} d_{v,i}[n]$.

  Note that such further division of $c_i[n]$ and $d_i[n]$ into different parts is a logical approach to capture the charging and discharging of a PHEV.

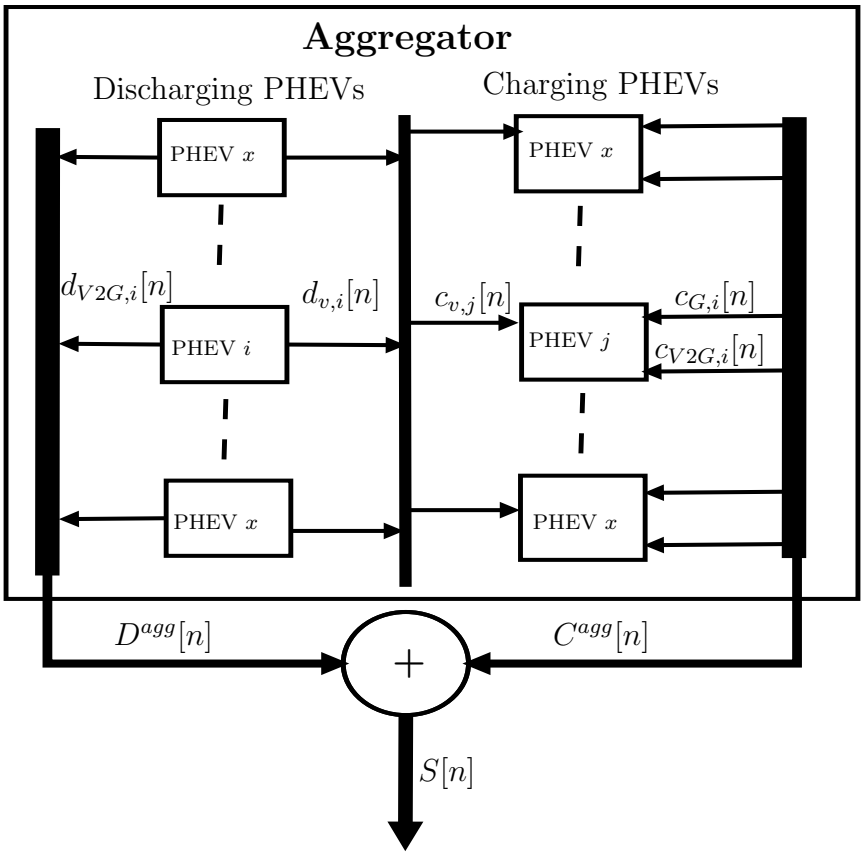

Figure 3.8: An illustration of a charging/discharging process within and to outside of the aggregator.

When $D^{agg}[n] > C^{agg}[n]$, $S[n]$ is greater than 0 and the aggregator provides power to the microgrid (backup service). When $D^{agg}[n] < C^{agg}[n]$, $S[n]$ is less than 0 and the aggregator absorbs power from the microgrid (storage service). When $S[n] = 0$, the aggregator does not provide any kind of service to the microgrid.

The aggregated charging and discharging rate are mainly subjected to two kinds of constraints. Firstly, the aggregator is constrained by a maximum possible current that can be transmitted through the aggregator [29]. Secondly, a situation of undervoltage may arise due to the the excessive loading from the aggregator in the distribution system, and vice cersa [47]. Such a situation imposes a constraint over the maximum aggregated charging

and discharging rate. Let C_{max}^{agg} be the maximum allowable aggregated charging rate of PHEVs, and D_{max}^{agg} be the maximum allowable aggregated discharging rate of PHEVs. The aggregated charging/discharging rate is constrained by the corresponding maximum rate and can be written as $0 \leq C^{agg}[n] \leq C_{max}^{agg}$ and $0 \leq D^{agg}[n] \leq D_{max}^{agg}$.

3.2 Research Problem

As discussed in Subsection 3.1.5, an energy transaction from one vehicle to an other vehicle is considered into the system model. Let *vehicle-to-vehicle (V2V) operation* define an energy transaction among the PHEVs within the aggregator. In this research, we focus on research problems that associate only with the V2V operation. The V2V operation transfers the energy from the source vehicles (which are parked for relatively longer times) to the destination vehicles (which are parked for relatively shorter times). The depleted energy of the source vehicles is fulfilled by the surplus RES supply in the future which shows that the V2V operation becomes beneficial only when there is a surplus RES supply in the future. On the other hand, the V2V operation also enables the V2G system to absorb an additional amount of surplus RES energy (in contrast to the case when the V2V operation is not adopted) in the future, thereby enhancing the storage capability of the V2G system. Moreover, it is also true that the energy imported from the utility grid (when a set of PHEVs demands for the charging) is also minimized, thereby enhancing the RES penetration.

Microgrid Operation Scenarios

We divide the microgrid operation into nine different scenarios based on the values of net microgrid load, $L_N[n]$, and net power supplied by the aggregator, $S[n]$. The $L_N[n]$ can be at three different states ($L_N[n] > 0$, $L_N[n] < 0$, and $L_N[n] = 0$). For each state of $L_N[n]$, $S[n]$ can have three different states ($S[n] > 0$, $S[n] < 0$, and $S[n] = 0$). Overall, the combinations of $L_N[n]$ and $S_N[n]$ yield the nine different scenarios. Each scenario restricts the state (positive, negative, N/A, or zero) of variables $c_{V2G,i}[n]$, $d_{V2G,i}[n]$, $c_{v,i}[n]$, $d_{v,i}[n]$, and $c_{G,i}[n]$. The possible nine scenarios of the microgrid operation with the corresponding state of the variables are shown in Table 3.1, where $i \in \{1, 2, ..., I\}$ and $n \in \{1, 2, ..., N\}$. The table also shows that a V2V operation is possible only in the scenario when $L_N[n] < 0$ and $S[n] < 0$ i.e., only when the V2G system is providing the storage service. This shows that the V2V operation is executed on the top of the V2G system. When the rates $d_{v,i}[n] > 0$ or $c_{v,i}[n] > 0$ then there exist a V2V operation at time-slot n. Recall that $d_{v,i}[n]c_{v,i}[n] = 0$. When there is a V2V operation, $\sum_{i=1}^{I} c_{v,i}[n] = \sum_{i=1}^{I} d_{v,i}[n]$ must be true. This implies that the power discharged by a set of PHEVs, for the purpose of the V2V operation, must be consumed by a set of PHEVs within the aggregator. Such discharging ($d_{v,i}[n]$) and charging ($c_{v,i}[n]$) components have no effect in the computation of $S[n]$.

Research Problem

The V2V operation can be possible only when the overall charging demand from PHEVs within the aggregator is greater than the total supply provided by the excess RES ($L_N[n] < 0$). In this research, we focus on making decisions such as whether or not a V2V operation

Table 3.1: Scenarios of the microgrid operation.

Net Load	Aggregator's net power supply	$c_{V2G,i}[n]$	$d_{V2G,i}[n]$	$c_{v,i}[n]$	$d_{v,i}[n]$	$c_{G,i}[n]$	Remarks
$L_N[n] > 0$ (Backup Service)	$S[n] = 0$	$= 0$[a]	$= 0$	$= 0$[c]		$= 0$	
	$S[n] > 0$*		> 0			≥ 0	$\sum_{i=1}^{I} d_{V2G,i}[n] > \sum_{i=1}^{I} c_{G,i}[n]; \forall n$
	$S[n] < 0$		≥ 0			> 0[d]	$\sum_{i=1}^{I} d_{V2G,i}[n] < \sum_{i=1}^{I} c_{G,i}[n], \forall n$
$L_N[n] < 0$ (Storage Service)	$S[n] = 0$	$= 0$	$= 0$[b]	$= 0$[c]		$= 0$	
	$S[n] > 0$	N/A		N/A			N/A
	$S[n] < 0$**	≥ 0		≥ 0	≥ 0	≥ 0[d]	$\sum_{i=1}^{I} c_{v,i}[n] = \sum_{i=1}^{I} d_{v,i}[n]; \forall n$ #
$L_N[n] = 0$	$S[n] = 0$	$= 0$[a]	$= 0$[b]	$= 0$[c]		$= 0$	
	$S[n] > 0$			N/A			N/A
	$S[n] < 0$			$= 0$[c]		≥ 0[d]	

* Provides Backup service

** Provides Storage service

[a] No charging from V2G operation i.e., No RES charging of PHEVs

[b] No discharging to V2G Operation i.e., Microgrid Load is not served with V2G operation

[c] V2V operation is not considered. i.e., No power transaction among the PHEVs

[d] a group of PHEVs acting as a load

\# the only scenario where V2V operation is considered.

should be invoked, and if there is a V2V operation then how a PHEV should participate in the V2V operation. The decisions are made on per-PHEV basis.

Consider a V2V operation at time-slot n ($L_N[n] < 0$, $S[n] < 0$ and $|S[n]| > |L_N[n]|$). For a certain additional demand of battery charging from a set of PHEVs ($|S[n]| - |L_N[n]|$) in the parking lot, we want to find the answers to the following two questions:

Question 1: Should PHEV i discharge in a given V2V operation for a given time-slot n or not?, and

Question 2: If PHEV i should discharge in the V2V operation, what is the maximum power that PHEV i is allowed to discharge for the V2V operation?

3.3 Problem Formulation

3.3.1 Research Question 1

To determine whether or not PHEV i should discharge in a given V2V operation for a given time-slot n, we take a threshold based approach. We define a certain threshold, Ω, and compute a metric, $\omega_i[n]$, for PHEV i at time-slot n. If $\omega_i[n] > \Omega$, PHEV i should discharge its battery otherwise PHEV i should not discharge, but should charge, in the V2V operation. A PHEV should discharge its battery only when it has enough charge in its battery and is going to stay in the parking lot for a longer time. In such case, the PHEV battery can be charged again in following time-slots when there is a surplus RES supply. This should enhance the aggregated storage capacity in later time-slots, thereby utilizing RES more. Hence, the metric, $\omega_i[n]$, should depend on the values of $SOC_i[n]$ and $\tau_i[n]$. Define two thresholds:

- $SOC_\Omega-$SOC threshold for PHEV i such that, if $SOC_i[n]$ is below the threshold, the metric, $\omega_i[n]$ is equal to ω_{min}; and
- $\tau_\Omega-$ time threshold for PHEV i such that, if $SOC_i[n]$ is below the threshold, the metric, $\omega_i[n]$ is equal to ω_{min},

where,

$$\omega_{min} = \alpha_{soc} SOC_\Omega + \alpha_\tau \frac{\tau_\Omega}{\tau_{max}}, \tag{3.9}$$

α_{soc} and α_τ are weights given to SOC and τ of PHEV respectively. Note that $\alpha_{soc}+\alpha_\tau = 1$. The $\omega_i[n]$ is computed as

$$\omega_i[n] = \begin{cases} \omega_{min}, & SOC_i[n-1] \leq SOC_\Omega \text{ or } \tau_i[n] \leq \tau_\Omega \\ \alpha_{soc} SOC_i[n-1] + \alpha_\tau . \dfrac{\tau_i[n]}{\tau_{max}}, & \text{otherwise,} \end{cases} \tag{3.10}$$

where, τ_{max} is the maximum possible time that a PHEV is plugged-in and $\omega_i[n] \in [\omega_{min}, 1]$. Finally, PHEV i should discharge in a V2V operation when $\omega_i[n] \geq \Omega$, where, $\Omega \in [\omega_{min}, 1]$. The number of PHEVs which are discharging in a V2V operation directly depends upon the value of threshold Ω, and increases with a decrease in the Ω value. This implies that, when $\Omega = \omega_{min}$, then there will be the maximum possible number of PHEVs that are discharging in a V2V operation. Similarly, when $\Omega = 1$, then there will be no PHEVs that are discharging in a V2V operation at all.

In this research, we aim at resolving the optimum value of α_{soc} (thereby the optimal value of α_τ) that maximizes the total amount of energy discharged in a V2V operation. It will also satisfy that no PHEV battery is depleted below its initial SOC when it leaves the parking lot at an expected time. Similarly, the value of SOC_Ω and τ_Ω should not be chosen too low such that a PHEV battery may be depleted below its initial SOC when it leaves the parking lot at an expected time. In this research, we arbitrary choose the values of SOC_Ω and τ_Ω.

In summary, a PHEV i should discharge in a V2V operation only when $\omega_i[n] \geq \Omega$, where, $\Omega \in [\omega_{min}, 1]$, $\omega_i[n] \in [\omega_{min}, 1]$.

3.3.2 Research Question 2

To determine the maximum energy that PHEV i should discharge for the V2V operation; we study how it should depend on the current metric, $\omega_i[n]$, and the maximum amount of energy that PHEV i can discharge for the V2V operation. Let $\overline{d_{v,i}[n]}$ denote the maximum energy that can be discharged from PHEV i for the V2V operation at time-slot n. The maximum amount of energy, in PHEV i, available for discharging in the V2V operation is the excess amount of energy above the threshold SOC_Ω. It is computed based on the threshold SOC_Ω and SOC of PHEV i battery at previous time-slot, $SOC_i[n-1]$, the amount of energy in the battery at the beginning of time-slot n is given by $e(SOC_i[n-1]-SOC_\Omega)$. The maximum energy that can be discharged from PHEV i at time-slot n is the fraction of the maximum amount of energy available for discharge as given by the metric, $\omega_i[n]$. Hence,

$$\overline{d_{v,i}[n]} = e \cdot (SOC_i[n-1] - SOC_\Omega) \cdot \eta_d \cdot \omega_i[n]. \tag{3.11}$$

However, $d_{v,i}[n] \leq min(D^{max} - d_{V2G,i}[n], \overline{d_{v,i}[n]}) = min(D^{max}, \overline{d_{v,i}[n]})$ because $L_N[n] < 0$ i.e., the V2G system is in the storage service mode, thereby $d_{V2G,i}[n] = 0$. Recall that D^{max} is the maximum allowable discharging rate of a PHEV battery.

3.3.3 Necessary and Sufficient Conditions for V2V Operation

In order to invoke a V2V operation, both the necessary and the sufficient conditions need to be satisfied. As discussed in Section 3.2, we consider a V2V operation only during a V2G storage service ($L_N[n] < 0$). The main objective of the V2V operation is to minimize

the power import from the utility grid for charging a set of PHEVs during a V2G storage service.

The Necessary condition

As discussed in Section 3.1, it is desired that the MGCC charge all the PHEV batteries fully or as much as possible before they depart from the parking lot. On the other hand, MGCC should guarantee that a PHEV is not discharged below its initial energy level $\overline{x_i}$ before it departs (given that PHEV i stays in parking spot i for entire occupancy M_i). Hence, at each time-slot n, PHEV i demands a minimum charging rate, denoted as $\delta_{i,min}[n]$, given by

$$\delta_{i,min}[n] = \frac{e - x_i[n-1]}{\tau_i[n]}. \tag{3.12}$$

In time-slot n, if the total minimum demand of all PHEVs, $\sum_{i=1}^{I} \delta_{i,min}[n]$, is greater than the surplus RES supply, $L_N[n]$, an extra amount of power $(\sum_{i=1}^{I} \delta_{i,min}[n] - L_N[n])$ has to be imported from the utility grid. The V2V operation will be invoked in such a condition to minimize the power imported from the grid. The necessary condition for a V2V operation is summarized as follows

$$\sum_{i=1}^{I} \delta_{i,min}[n] > L_N[n]. \tag{3.13}$$

The Sufficient Condition

In order to determine a sufficient condition, first we divide the PHEVs into two groups, namely, a set of charging PHEVs ($\Psi_{c,n}$) and a set of discharging PHEVs ($\Psi_{d,n}$). The total minimum charging demand by PHEV set $\Psi_{c,n}$ is $sum_{cv,n} = \sum_{i \in \Psi_{c,n}} \delta_{i,min}[n]$. If the total minimum charging demand $sum_{cv,n}$ is not satisfied by the excess RES supply ($|L_N[n]|$), and there is a number of PHEVs ready to discharge in the V2V operation, then V2V operation will be invoked.

In order to determine sets $\Psi_{c,n}$ and $\Psi_{d,n}$ at time-slot n, first we compute the metric $\omega_i[n]$. If $\omega_i[n] \geq \Omega$, PHEV i is assigned to set $\Psi_{d,n}$, otherwise, PHEV i is assigned to set $\Psi_{c,n}$. Hence, the sufficient condition to initiate a V2V operation is

$$\sum_{i \in \Psi_{c,n}} \delta_{i,min}[n] > L_N[n] \text{ and } \Psi_{d,n} \neq \emptyset. \tag{3.14}$$

3.3.4 V2V Operation Revenue and Cost

The V2V operation helps in reducing the total amount of energy imported from the utility grid, thereby enhancing the RES penetration into the microgrid. The equivalent reduction in the energy import from the utility is regarded as the revenue of the V2V operation. Similarly, the V2V operation causes some unwanted energy conversion loss during the energy transaction within the parking lot which is regarded as the cost of the V2V operation. We measure the V2V operation operation cost and revenue in terms of an amount of energy. In this subsection we explain the V2V operation cost and revenue in details.

Revenue

As discussed earlier, the V2V operation helps in reducing the energy import from the utility grid. In other words, the V2V operation enhances the storage-capacity of the V2G system. The amount of discharge energy in the V2V operation in a given time-slot provides the equivalent amount of enhanced storage-capacity of the V2G system in the future time-slots. Hence, when there exists a surplus RES supply in the future the enhanced storage-capacity of the V2G system is utilized by storing the surplus RES energy supply. In this way the amount equivalent to the enhanced storage-capacity of the V2G system is reduced in importing from the utility grid. We consider such equivalent amount of energy to be the benefit due to the V2V operation. This shows that the revenue of the V2V operation is equal to the total amount of energy that is successfully transferred to charging PHEVs via V2V operation. Denote R as the total amount of revenue due to V2V operation over time horizon T. R is computed as the total amount of energy charged due to $c_{v,i}[n]$ for all PHEVs over the time horizon T, is given by

$$Rv = \sum_{i=1}^{N} \sum_{i=1}^{I} c_{v,i}[n]\Delta. \tag{3.15}$$

The total amount of energy transferred to the charging PHEVs via V2V operation is equivalent to the total amount of energy deducted from the utility grid.

Cost

When a PHEV demands for the extra energy over the energy supplied by the RES, the demand can be fulfilled either by importing the power form the grid or by the V2V operation. When a PHEV is charged by the grid, the process suffers from only one energy conversion loss (during charging of the PHEV battery). However, when a PHEV is charged

by the V2V operation, the process incurs two energy conversion losses (discharging a source PHEV and then charging a destination PHEV). This clearly explains that charging a destination PHEV by the V2V operation causes an extra energy conversion loss (due to the discharging of a source PHEV). We consider the additional energy conversion loss to be the cost of the V2V operation.

The cost incurred when PHEV i discharges at time-slot n is the difference of the energy before and after a discharge of the discharging PHEV in the V2V operation which is given as, $z - d_{v,i}[n]\Delta = (\frac{d_{v,i}[n]}{\eta_d} - d_{v,i}[n])\Delta = d_{v,i}[n](\frac{1-\eta_d}{\eta_d})\Delta$, where, z is the corresponding amount of energy in a discharging-PHEV's battery before the discharge. The corresponding discharged amount is $d_{v,i}[n]$ at time-slot n.

Finally, the total cost of the V2V operation over time horizon T, denoted by U, is the sum of the cost incurred due to all PHEVs in the parking lot given by

$$U = \left(\frac{1-\eta_d}{\eta_d}\right) \sum_{n=1}^{N} \sum_{i=1}^{I} d_{v,i}[n]\Delta. \tag{3.16}$$

Moreover, when there is not a sufficient surplus RES supply in the future, the total amount of the energy depleted from the discharging PHEVs is compensated by the utility grid instead of the surplus RES supply. In this situation the V2V operation appears to be ineffective. A PHEV, which is expected to stay a long time in a parking lot, agrees to discharge in the V2V operation with an expectation to charge its battery from RES in the future. Hence, the discharged power is expected to be fulfilled by the RES supply. If RES supply in the future cannot be provided then energy that had been transferred out for the V2V operation need to be compensated by the utility grid. In conclusion, we can say that

the V2V operation, over time horizon T, becomes ineffective when the total amount of energy transaction in the V2V operations exceeds the total amount of energy delivered by the surplus RES supply. More formally, when $\sum_{n=1}^{N}\sum_{i=1}^{I} d_{v,i}[n]\Delta > \sum_{n=1}^{N}\sum_{i=1}^{I} c_{V2G,i}[n]\Delta$ the V2V operation is not beneficial.

3.3.5 Research Issues and Objectives

This research is dedicated to study the novel V2V operation which enhances the storage capacity of the V2G system, thereby enhancing the RES penetration for sufficient surplus RES supplies. Subsection 3.3.3 explains the necessary and sufficient conditions to invoke a V2V operation. As explained in the subsection, once the necessary condition for a V2V operation at time-slot n is satisfied, the values of threshold Ω and metric $\omega_i[n]$ determine whether or not PHEV i, at time-slot n, should discharge for a V2V operation. The research issues are related to the methods of resolving the values of Ω and $\omega_i[n]$ for the V2V operation.

In a V2V operation, there are two sets of PHEVs, namely the set of charging PHEVs, Ψ_c, and the set of discharging PHEVs, Ψ_d. It is desirable that the total number of PHEVs, in the parking lot, be divided into sets Ψ_c and Ψ_d in such a way that the energy transaction in the V2V operation is maximized. It will also satisfy the condition that the final SOC (the SOC of a PHEV before it leaves the parking lot at an expected time) of any PHEV do not go below the initial SOC. The division of total number of PHEVs into Ψ_c and Ψ_d depends upon the values of Ω and $\omega_i[n]$, such division procedure needs to be carefully designed. This leads to the research issues which are related to the procedures of resolving the values

of Ω and $\omega_i[n]$ to maximize the V2V energy transaction while satisfying the PHEVs' SOC constraint.

When the value of $\Omega \in \{\omega_{min}, 1\}$ is equal to ω_{min}, the size of set Ψ_d is likely to grow relative to the size of set Ψ_c. This scenario may reduce the V2V energy transaction from the maximum possible value because of the relatively less charging demand with small size of set Ψ_c. Similarly, when $\Omega = 1$, set Ψ_d becomes a null set and there will be no V2V operation. Hence, there is a research issue to determine the optimal value of Ω that leads to the maximum energy transaction in the V2V operation. However, in this work we arbitrarily select a value of $\Omega \in \{\omega_{min}, 1\}$ and keep the value constant in order to limit the scope of the research.

The value of $\omega_i[n]$ determines the amount of energy transaction during the V2V operation at time-slot n. In (3.10), it is shown that the value of $\omega_i[n]$ for a given $SOC_i[n-1]$ and $\tau_i[n]$ can be controlled by varying the values of α_{soc} and α_τ. Hence, it is also a research issue to determine an optimal value of α_{soc} (recall that $\alpha_\tau = \alpha_{soc} - 1$) to maximize the V2V energy transaction while satisfying the PHEVs' SOC constraints for a given Ω over time horizon T. In this research, we only focus on resolving the value of weight α_{soc}, for a given Ω, that controls the value of $\omega_i[n]$.

Finally, the objective of this research is to analyze the impact of α_{soc} on the performance of the V2V operation. The performance of the V2V operation is measured on the basis of energy based metrics, namely V2V operation cost, U, and revenue, R. In order to analyze the impact, we run the simulation for different values of α_{soc} and observe the relationships between α_{soc} and R, and between α_{soc} and U. Moreover, we also observe the impact of unexpected PHEV departures on R and U by varying the value of the unexpected early

departure probability P_{th}.

3.4 Summary

In summary, we can say that the proposed novel V2V operation runs on the top of the V2G system. The V2V operation transfers the energy from the source vehicles to the destination vehicles, where the destination vehicles departs earlier than the source vehicles. The source vehicles stays longer and look to charge their batteries from the surplus RES supplies in the future. This shows that the V2V operation becomes ineffective if there are not sufficient surplus RES supplies in the future. Hence, the V2V operation enhances the storage-capacity of the V2G system, thereby creating an opportunity of enhancing the RES utilization.

It is always desirable that the V2V energy transaction is maximized satisfying the PHEVs' SOC constraint in which the final SOC of any PHEV should not go below corresponding initial SOC. The main parameters which control the V2V energy transaction are the threshold Ω, and the weight α_{soc}. In this research, we arbitrarily select the value of Ω and keep it constant while only the value of the weight α_{soc} is varied to analyze the impact of α_{soc} on the performance of the V2V operation. In addition, we also analyze the impact of earlier departures, with probability P_{th}, of vehicles than expected times on the performance of the V2V operation.

Chapter 4

Performance Evaluation

In this chapter, we study the impact of weight α_{soc} and probability P_{th} on the system performance parameters. The details of the system performance parameters are given in Section 4.2. We focus on obtaining the optimum value of α_{soc} such that the total energy transaction in the V2V operation (as given by the total V2V operation revenue, R) is maximized while satisfying PHEVs' SOC constraints. In addition, we observe the impacts on the other performance parameters such as overall RES utilization, total amount of backup and storage services etc. In order to observe such impacts, we build a simulator using a general purpose programming language C++, which has an object-oriented feature. The simulator implements the relationships between all the system variables explained in Chapter 3. In simulation, we vary the values of α_{soc} and P_{th}, and compute the values of performance parameters. The impact of α_{soc} and P_{th} on the performance parameters are analyzed based on the computed values.

4.1 Simulation Procedure

The microgrid system variables can broadly be classified into deterministic variables and random variables. Let a *simulation run* defines an instance of simulation that is executed over a time horizon. Variables that do not change (change) over different simulation runs are categorized as deterministic (random) variables. Let a *simulation scenario* defines a number of simulation runs for a given set of deterministic variables. In this research, the deterministic variables include load profile, $L[n]$, and mobility profile, M_i. The random variables include $R[n]$ and $Z_i[n]$. Note that, if $\tau_i[n] = 0$, a parking spot i is empty. If $\tau_i[n] = 1$, PHEV i will leave the parking spot i at the end of time-slot n. If $\tau_i[n] > 0$, a parking spot i is occupied at time-slot n.

The variables discussed above are input to the simulated microgrid system. The output variables in the simulated microgrid system are $G[n]$, $G_L[n]$, $c_i[n]$, $c_{V2G,i}[n]$, $c_{v,i}[n]$, $c_{G,i}[n]$, $d_i[n]$, $d_{v,i}[n]$, and $d_{V2G,i}[n]$. The output variables are updated at the end of time-slot n. In this research, we consider a simulation scenario with 5000 simulation runs.

Figure 4.1 demonstrates the flowchart for the simulation procedure. Refer Appendix A for detail algorithms used for the simulation.

4.2 Simulation Parameters

Consider the microgrid system deployed in a commercial or an industrial area, which is typically operated during a day time, e.g., from 6 a.m. to 9 p.m. in a day. This implies that the time horizon, T, is 15 hours. The duration of a time-slot (Δ) is chosen to be 10 minutes [27]. The total number of time-slots, $N = T \cdot (\text{total number of time-slots in an hour}) = 15 \cdot 6 =$

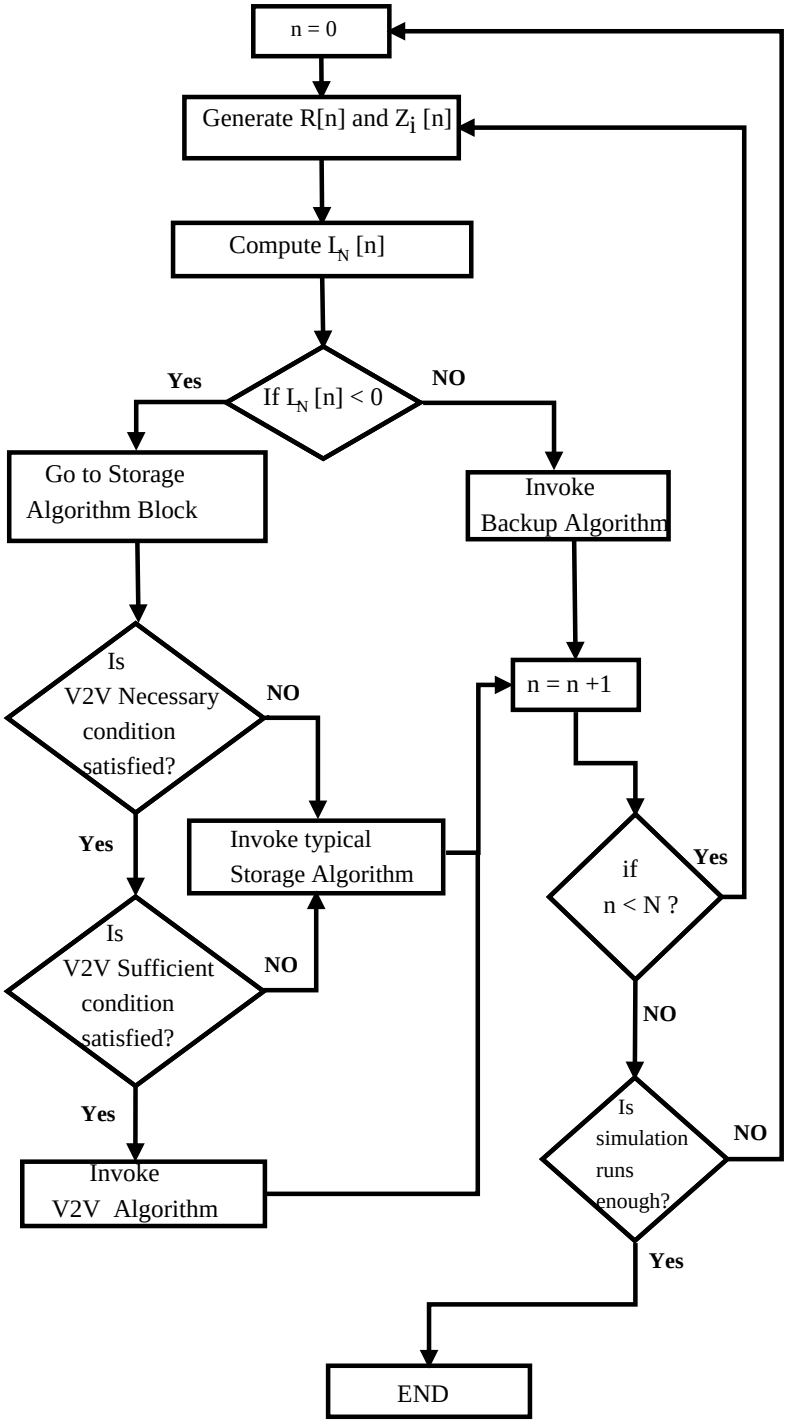

Figure 4.1: Flowchart to illustrate the overall simulation procedure.

90.

For simplicity, we consider only one typical load profile for the simulation, which is an industrial load profile from [11], with the peak load 1000 kW. The total number of parking spots, I, in the parking lot set to be 500. We consider that no parking spot remains empty for time horizon T. PHEV i arrives to parking spot i after traveling distance y_i, where y_i is uniformly distributed from 10 km to 70 km. PHEVs arrive within time-slots 1 to 30 (equivalently 6 a.m. to 11 a.m.) and depart within time-slots 55 to 85 (equivalently 3 p.m. to 8 p.m.). The arrival and departure time-slots are uniformly distributed within the corresponding range. The values of ranges are chosen arbitrarily, but representing the typical arrival and departure times. We consider only one mobility scenario.

A PHEV battery is depleted by $W = 0.15$ kWh for each km traveled [10]. All the PHEV batteries have same capacity, e, equal to 15 kWh. The PHEV battery charging efficiency, η_c, and discharging efficiency, η_d, are set to 0.9. Both maximum PHEV battery charging, C^{max}, and discharging rate, D^{max}, are set to 2.2 kWh. The self discharging rate, β, is 0.99. The utility grid can supply up to 1000 kW in a time-slot (i.e., $G_{max} = 1000$ kW). The nominal wind power is 1000 kW, and other parameters related to wind speed, namely cut-in wind speed, V_{ci}, rated wind speed, V_r, cut-out wind speed, V_{co}, are 3 m/s, 10 m/s, 20 m/s respectively. The forecast wind speed data are taken from the wind speed curve given in [10]. The total solar panel area is 1000 m^2 with a conversion efficiency of 0.2 [42]. The threshold for V2V operation, Ω, is set as 0.55. When we increase the value of Ω, the number of PHEVs discharging in V2V operation is decreased, and vice versa. The simulation has been performed for varied values of α_{soc} and P_{th}. Since $\alpha_{soc} + \alpha_\tau = 1$, when α_{soc} is increased, α_τ is correspondingly decreased. This refers that, when we increase the

value of α_{soc}, we give more priority to state-of-charge of PHEVs and less priority to the remaining time that a PHEV stays in the parking lot, in calculating metric $\omega_i[n]$. The simulation aims at determining optimum weights (α_{soc} and α_τ) for maximal performance. The performance is evaluated based on the performance metrics as explained in the following section.

4.3 Performance Metrics

The performance metrics are chosen to evaluate the performance of V2G services (storage service and backup service), V2V operation and RES utilization.

1. **Average PHEV battery SOC gain (Γ_{soc})**

   The metric provides a measure of overall average gain in SOC of all PHEV batteries. It is given by

   $$\Gamma_{soc} = \sum_{i=1}^{I} \frac{SOC_i[de_i] - SOC_i[a_i]}{1 - SOC_i[a_i]} \tag{4.1}$$

   where de_i is the departure time-slot of PHEV i.

2. **Ratio of RES supply over total supply (ϕ_{RES})**

   This metric measures the contribution made by RES supply in total supply to the microgrid. It is given by

   $$\phi_{RES} = \sum_{n=1}^{N} \frac{(R[n] - R_c[n])}{(R[n] - R_c[n]) + G[n]}. \tag{4.2}$$

3. **Total amount of storage energy (γ_S)**

It measures the total amount of energy supplied to all PHEVs by RES supply (storage service) over time horizon T. It is measured in kWh and given by

$$\gamma_S = \sum_{n=1}^{N} \sum_{i=1}^{I} c_{V2G,i}[n]\Delta. \tag{4.3}$$

4. **Total amount of backup energy (γ_B)**

   It measures the total amount of energy supplied by all PHEVs, providing backup service, to the typical microgrid load over time horizon T. It is measured in kWh and given as

$$\gamma_B = \sum_{n=1}^{N} \sum_{i=1}^{I} d_{V2G,i}[n]\Delta. \tag{4.4}$$

5. **Total energy from V2V charging (γ_{v2v})**

   It measures the total amount of entire PHEVs charging performed by the V2V operation over time horizon T. It is measured in kWh and given by

$$\gamma_{v2v} = \sum_{n=1}^{N} \sum_{i=1}^{I} c_{v,i}[n]\Delta. \tag{4.5}$$

   This metric evaluates the total amount of energy gained due to the V2V operation. The amount of energy would have been lost as RES curtailment in absence of the V2V operation. Hence, this metric evaluates the benefit from V2V operation.

6. **Total extra energy conversion loss due to V2V operation (ν_{v2v})**

   When a V2V operation is invoked, a PHEV is charged with an expense of extra energy conversion loss, which would not occur if the PHEV is directly charged from

the grid. The extra energy conversion is occurred due to the discharging of PHEVs during V2V operations. This metric gives the total energy conversion loss in time horizon T. It is measured in kWh and given by

$$\text{Total extra energy conversion loss due to V2V operation}, \nu_{v2v} = \frac{1-\eta_d}{\eta_d} \sum_{n=1}^{N} \sum_{i=1}^{I} d_i[n]\Delta. \tag{4.6}$$

This metric evaluates the total cost due to the V2V operation.

4.4 Evaluation of α_{soc} Impact

In simulation, the value of α_{soc} is varied from 0.1 to 0.9 with a step size of 0.1 to evaluate the impact of α_{soc}. Recall that a high value of α_{soc} corresponds to a low value of α_τ and vice versa, as given by relation $\alpha_{soc} + \alpha_\tau = 1$. For example, with $\alpha_{soc} = 0.9$ and $\alpha_\tau = 0.1$, the SOC of PHEV battery is given much higher priority in computation of metric $\omega_i[n]$ than remaining number of time-slots for PHEV to depart. Moreover, three different values of P_{th} as 0, 0.05 and 0.1 are considered in evaluating the α_{soc} impact. The simulation results demonstrates that α_{soc} has no impact on the average PHEV battery SOC gain (Γ_{soc}), ratio of RES supply over total supply (ϕ_{soc}), total amount of storage energy (γ_S) and total amount of backup energy (γ_B). On the other hand, the total energy from V2V charging (γ_{v2v}) and total extra energy conversion loss due to V2V operation (ν_{v2v}) increase with an increasing value of α_{soc}. Nevertheless, such increment is significant only for $P_{th} = 0$, i.e., when PHEVs do not depart early from the parking lot.

Impact on average PHEV battery SOC gain (Γ_{soc})

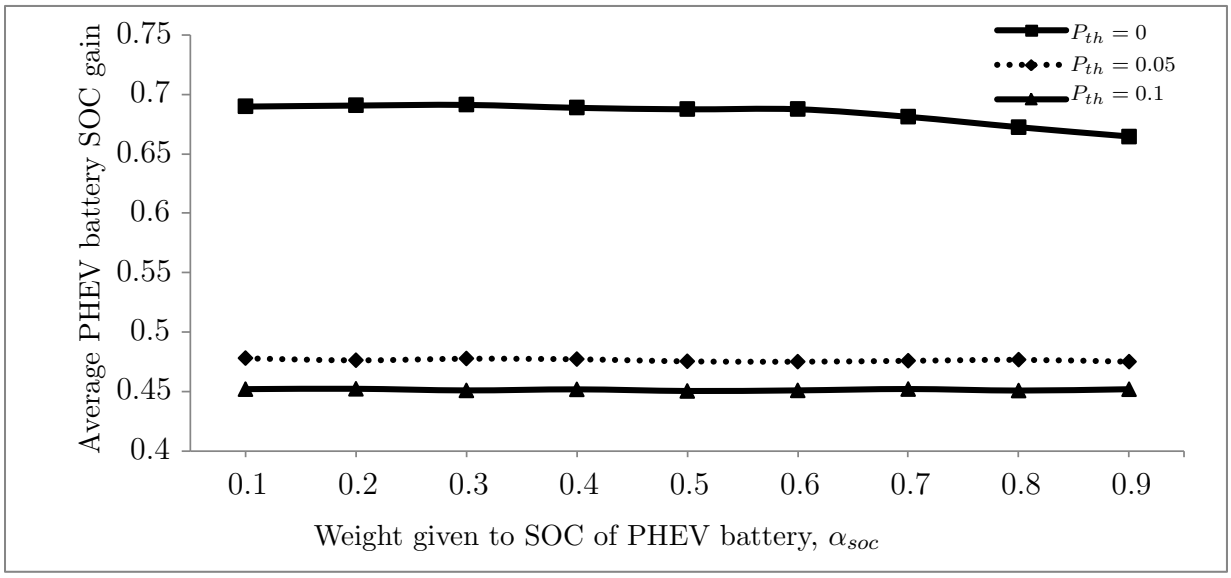

Figure 4.2: Average PHEV battery SOC gain.

For the impact on the final SOC of PHEVs before they depart from the parking lot, Figure 4.2 depicts the average PHEV battery SOC gain (Γ_{soc}). The variation of α_{soc} has almost no impact on Γ_{soc}. Nevertheless, the overall value of Γ_{soc} decreases abruptly when P_{th} increases from 0 to 0.05, and continues decreasing for the further increase in P_{th}. However, there is a slight decrease in Γ_{soc} as α_{soc} is set around 0.7 (for $P_{th} = 0$) as shown in Figure 4.2. This is caused by the increase in the discharging amount of energy in V2V operation, as discussed in the following.

Impact on Ratio of RES supply over total supply (ϕ_{RES})

In order to study the impact on RES contribution to the microgrid load, the ratio of RES supply over total supply (ϕ_{RES}) versus α_{soc} is shown in Figure 4.3. The curves are almost constant for the different values of α_{soc}. However, the overall ϕ_{RES} gradually decreases for an increasing value of P_{th} as observed from Figures 4.3.

Impact on total amount of storage energy (γ_S) and total amount of backup energy (γ_B)

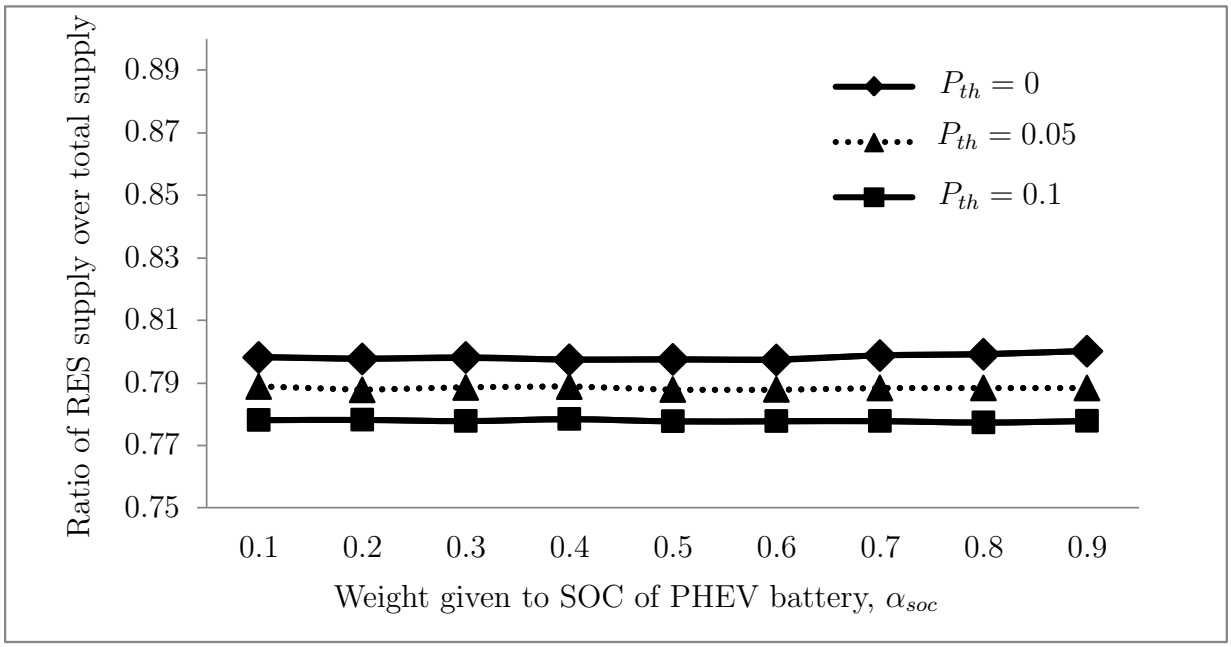

Figure 4.3: Ratio of RES supply over total supply.

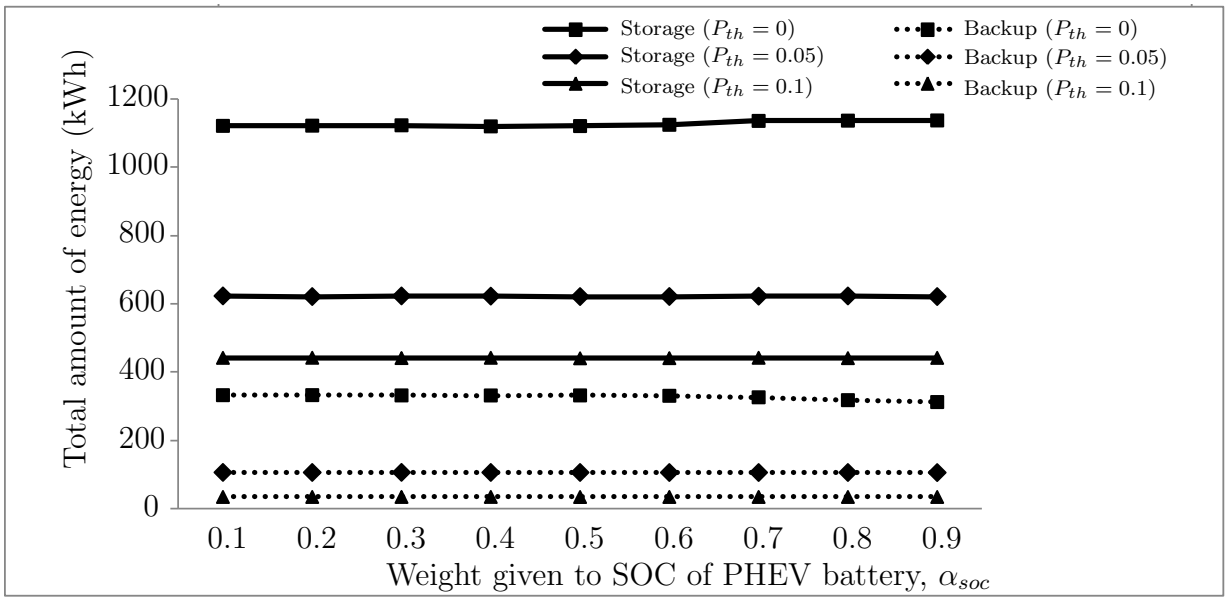

Figure 4.4: Total amount of storage and backup energy.

Figure 4.4 demonstrates how the total amount of storage energy (γ_S) and total amount of backup energy (γ_B) vary with α_{soc}. The curves are insensitive with the variation of α_{soc}. However, both γ_S and γ_B are almost halved when P_{th} is increased from 0 to 0.05, and they continue to decrease for $P_{th} = 0.1$. Moreover, γ_S is always greater than γ_B, because the algorithm never lets the SOC of PHEVs' battery go below the corresponding initial SOC and there is surplus RES energy for the scenario under consideration.

Impact on total energy from V2V charging (γ_{v2v}) and total extra energy conversion loss due to V2V operation (ν_{v2v})

In order to study the impact on cost and benefit of adopting V2V operation, Figure 4.5 shows total energy from V2V charging (γ_{v2v}), which is the V2V benefit, and the total extra energy conversion loss due to V2V operation (ν_{v2v}), which is the V2V cost, versus α_{soc}. The benefit and cost are sensitive to α_{soc} only when $P_{th} = 0$. The total amount of energy starts to increase mainly when α_{soc} is larger than 0.5 (i.e., more priority is given to SOC of PHEV in contrast to remaining time of PHEV's stay in parking lot, $\tau_i[n]$). The values of γ_{v2v} and ν_{v2v} reach the peaks when $\alpha_{soc} = 0.8$. The main reason of an increased γ_{v2v} for prioritized α_{soc} over α_τ is that SOC of PHEVs' battery tends to increase, while, $\tau_i[n]$ monotonically decreases over time horizon T. Hence, the metric $\omega_i[n]$ is likely to cross the threshold, Ω, more often for an increased α_{soc}, which means more PHEVs are discharging in V2V operation, thereby increasing the value of γ_{v2v}.

The peak values of γ_{v2v} and ν_{v2v} are around 100 kWh and around 10 kWh, respectively. The value of γ_{v2v} is always greater than ν_{v2v}, because the discharged amount of energy during V2V operation is mostly compensated by surplus RES energy, under the considered scenario, over time horizon T.

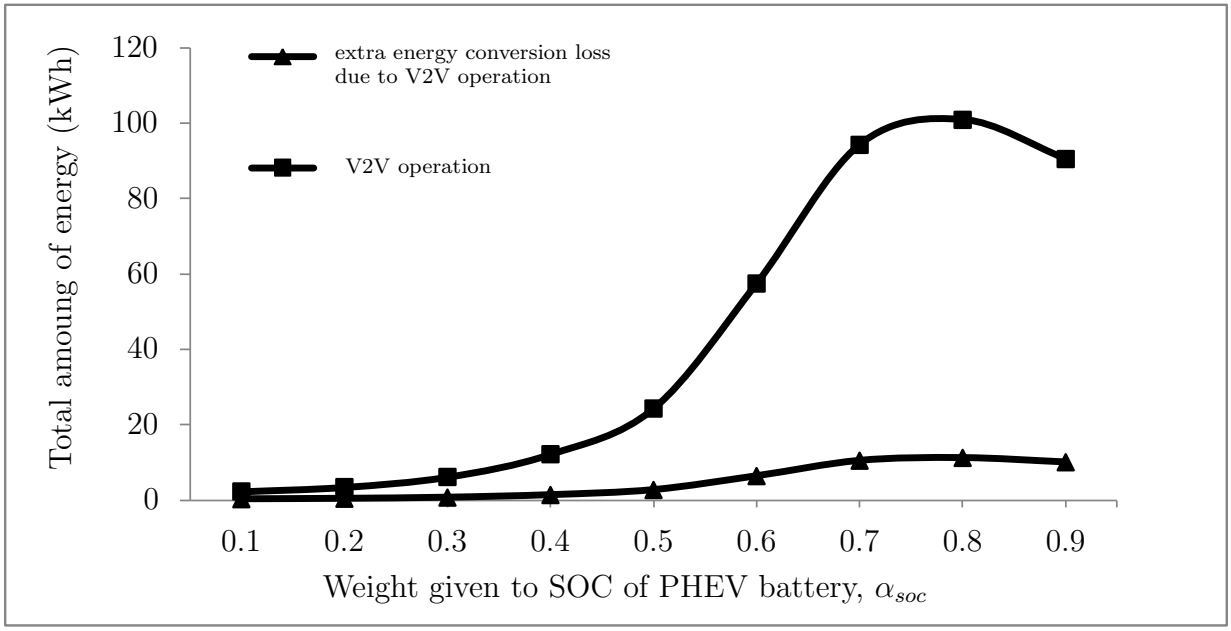

(a) $P_{th} = 0$.

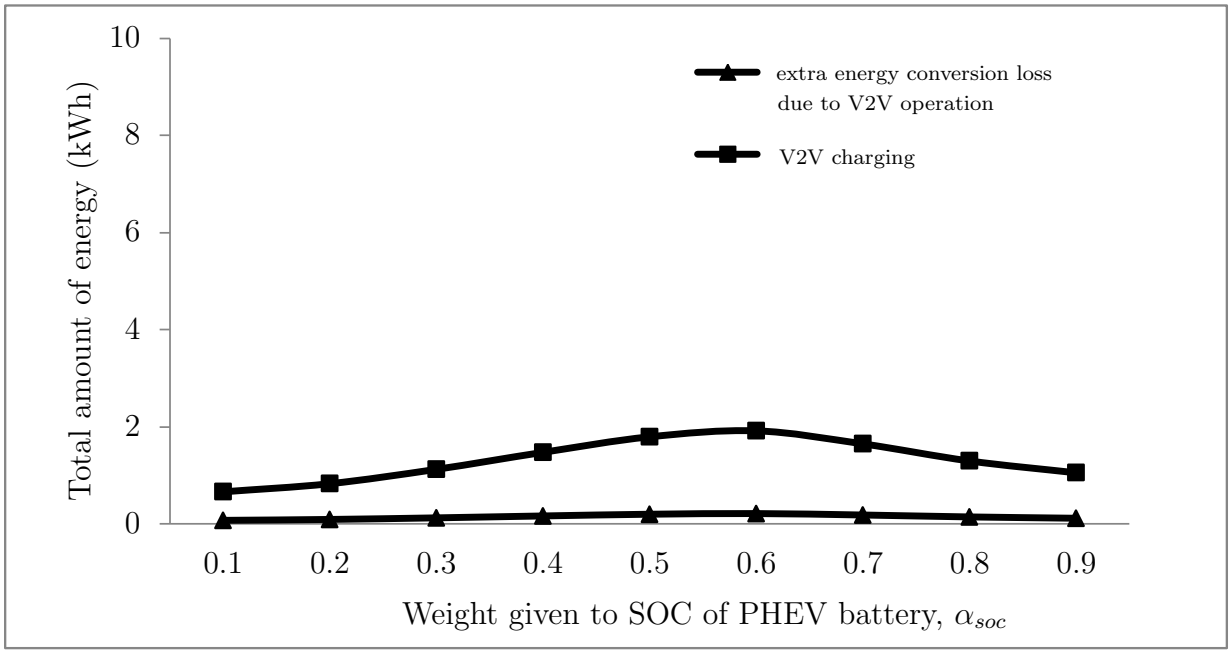

(b) $P_{th} = 0.05$.

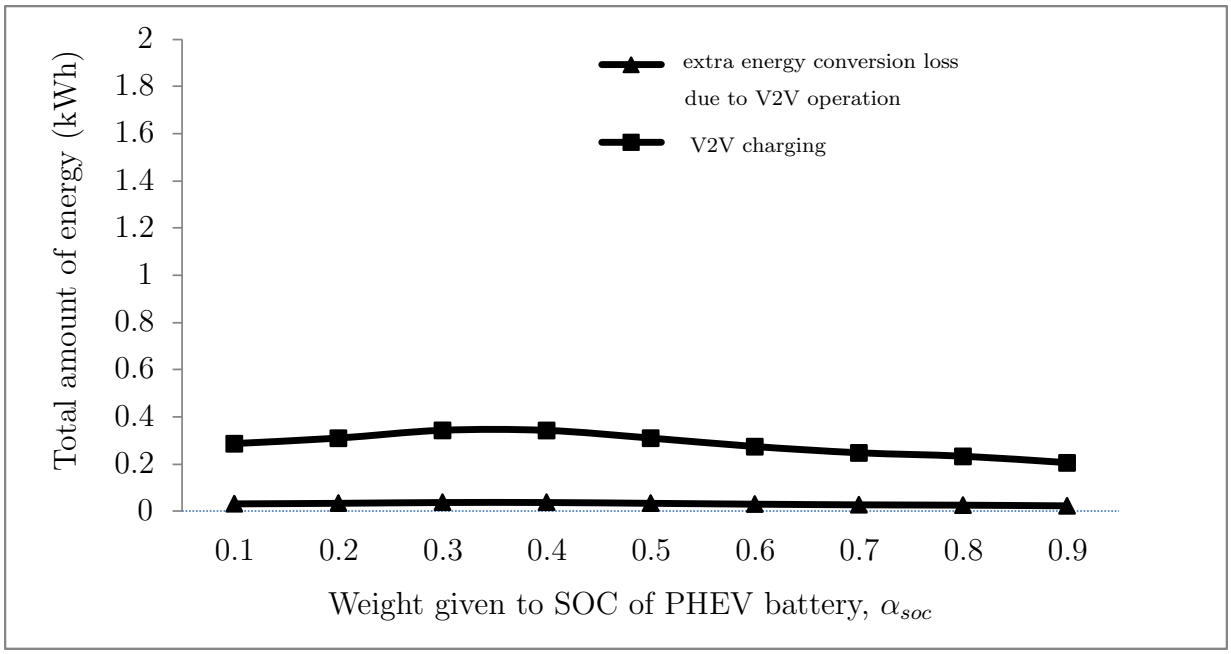

(c) $P_{th} = 0.1$.

Figure 4.5: Total amount of energy from V2V charging and Total extra energy conversion loss due to V2V operation.

Conclusion

From simulation results, the total energy from V2V charging (V2V operation benefit) is always greater than the total extra energy conversion loss due to V2V operation (V2V operation cost). The benefit starts increasing from $\alpha_{soc} = 0.6$ and peaks at $\alpha_{soc} = 0.8$ with a value of around 100 kWh. The value is nearly 10% of γ_S. However, such an increment exists for $P_{th} = 0$ only (i.e., no PHEVs departs early). For early departure of only 5% PHEVs, the increment in α_{soc} has almost no impact on the values of benefit. Moreover, when the benefit peaks to value of around 100 kWh, the value of cost is only around 10 kWh. That is, the V2V operation cost is only around 10% of the V2V operation benefit, which is very encouraging performance.

4.5 Evaluation of P_{th} Impact

In simulation, the value of P_{th} is varied from 0 to 0.1 with a step size of 0.025 to evaluate the impact of P_{th}. As an illustration $P_{th} = 0$ implies that no PHEV departs early from the predetermined departure time (as determined in the mobility scenario). Similarly, $P_{th} = 0.1$ implies that a PHEV independently departs early with 10% of chances. It can also be referred as 10% of PHEVs departs early from the parking lot. The impact of varied P_{th} is evaluated from three different values of α_{soc}, 0.1, 0.5 and 0.9.

The simulation results show that P_{th} has an impact on all the performance metrics different from α_{soc}. There exists a reverse impact on the performance metrics for increasing value of P_{th}. As discussed Section 4.4, there is a relative increment in the overall value of total energy from V2V charging (γ_{v2v}) with $\alpha_{soc} = 0.5$ and 0.9, which is consistent with the results given in the following.

Impact on average PHEV battery SOC gain (Γ_{soc})

In order to study the impact on the final SOC of PHEVs before they depart from the parking lot, Figure 4.6 demonstrates the average PHEV battery SOC gain (Γ_{soc}) for $\alpha_{soc} = 0.1$, 0.5, and $\alpha_{soc} = 0.9$. The curves abruptly decline when P_{th} increases from 0 to 0.025 and gradually decreases with an increasing value of P_{th}. The decrement comes from that a PHEV will miss the opportunity of charging due to its early departure. On the other hand, the curves are almost the same for $\alpha_{soc} = 0.1$ and 0.5, while, there is a slight decrease in overall results when $\alpha_{soc} = 0.9$.

Impact on ratio of RES supply over total supply (ϕ_{RES})

The ratio of RES supply over total supply (ϕ_{RES}) gradually decreases with an increasing

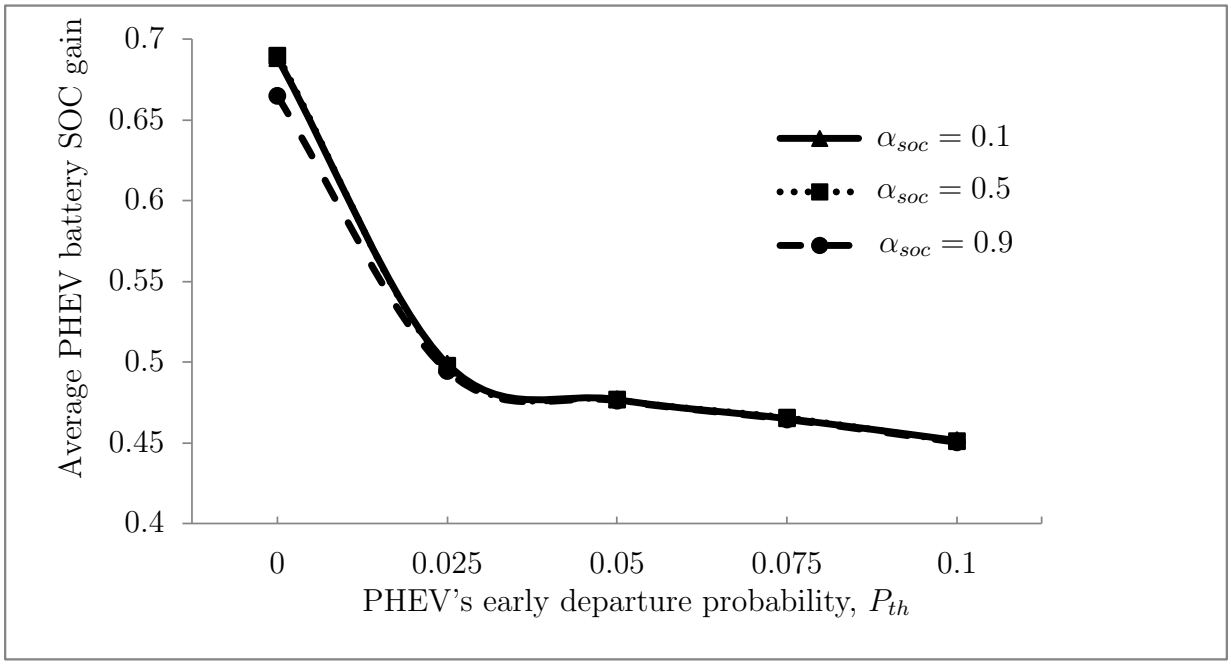

Figure 4.6: Average PHEV battery SOC gain.

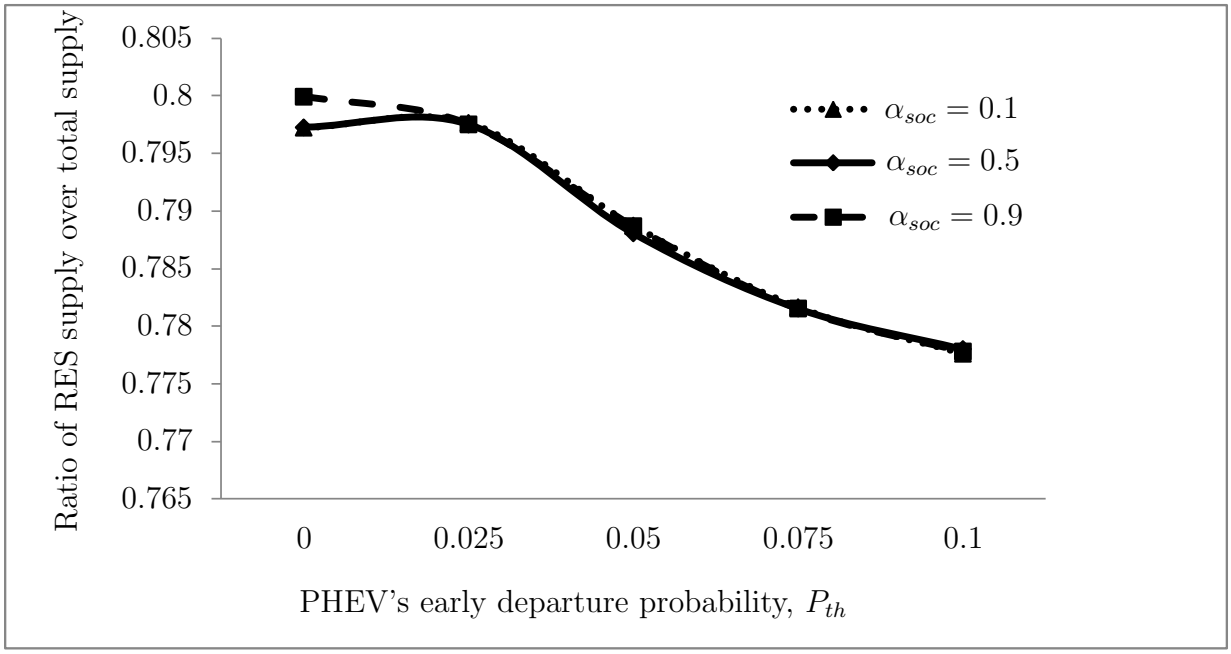

Figure 4.7: Ratio of RES supply over total supply.

value of P_{th}. When PHEVs depart early, the opportunities of storage and backup operation are decreased, thereby decreasing the values of γ_S and γ_B. Decreasing values of γ_S and γ_B corresponds to a decreased value of ϕ_{RES}.

Impact on total amount of storage energy (γ_S) and total amount of backup energy (γ_B)

The total amount of storage energy (γ_S) and total amount of backup energy (γ_B) monotonically decrease with an increasing value of P_{th}, as shown in Figure 4.8. However, the plots γ_S and γ_B do not change with the variations in α_{soc} value. As the number of early departing PHEVs increases (with an increase in the P_{th} value) the number of PHEVs for V2G operation is relatively decreased. Hence, the values of γ_S and γ_B decrease.

Impact on total energy from V2V charging (γ_{v2v}) and total extra energy conversion loss due to V2V operation (ν_{v2v})

The impact of early departure PHEVs on both total energy from V2V charging (γ_{v2v}) and total extra energy conversion loss (ν_{v2v}) is shown in Figure 4.9. The curves decline with an increasing value of P_{th}. However, it is significant only when $\alpha_{soc} = 0.9$. The level of curves increases with the α_{soc} value. As discussed earlier, the value of ν_{v2v} is always less than that of γ_{v2v}. Similarly, the peak values of γ_{v2v} and ν_{v2v} are obtained when $\alpha_{soc} = 0.9$ and $P_{th} = 0$.

Conclusion

As shown in the simulation results, the performance metrics, namely average PHEV battery SOC gain, total energy from V2V charging and total extra energy conversion loss due to V2V operation decrease abruptly when P_{th} increases from 0 to 0.025 and gradually decreases for a further increment in P_{th}. On the other hand, the performance metrics,

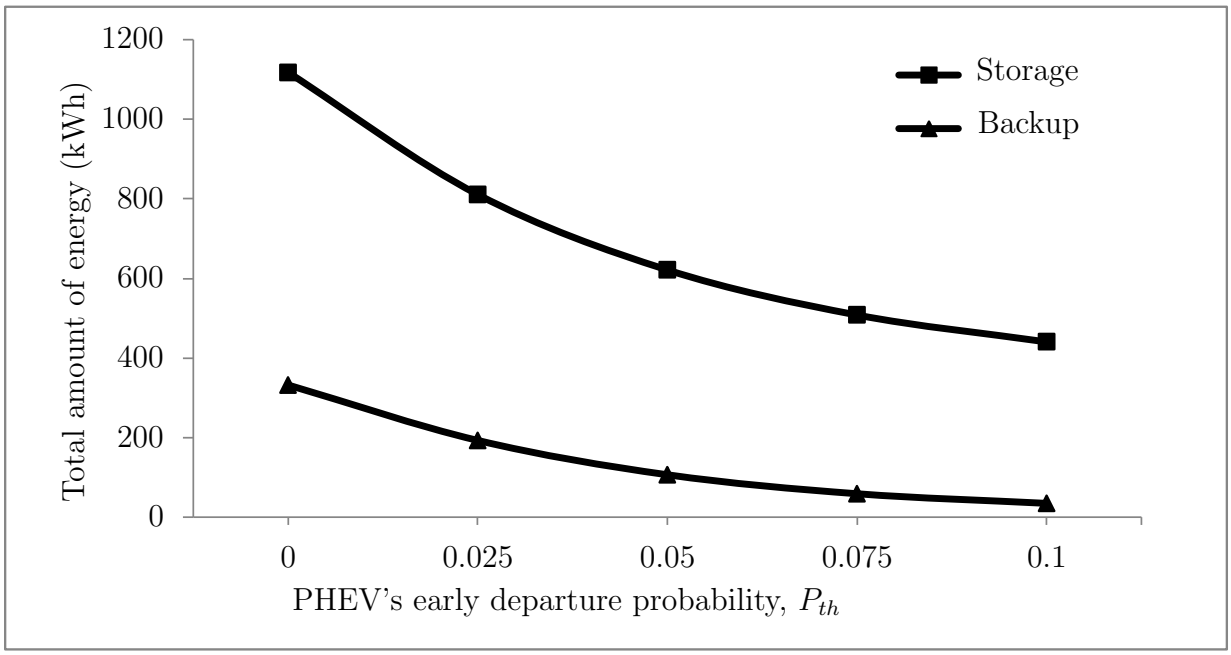

(a) $\alpha_{soc} = 0.1$.

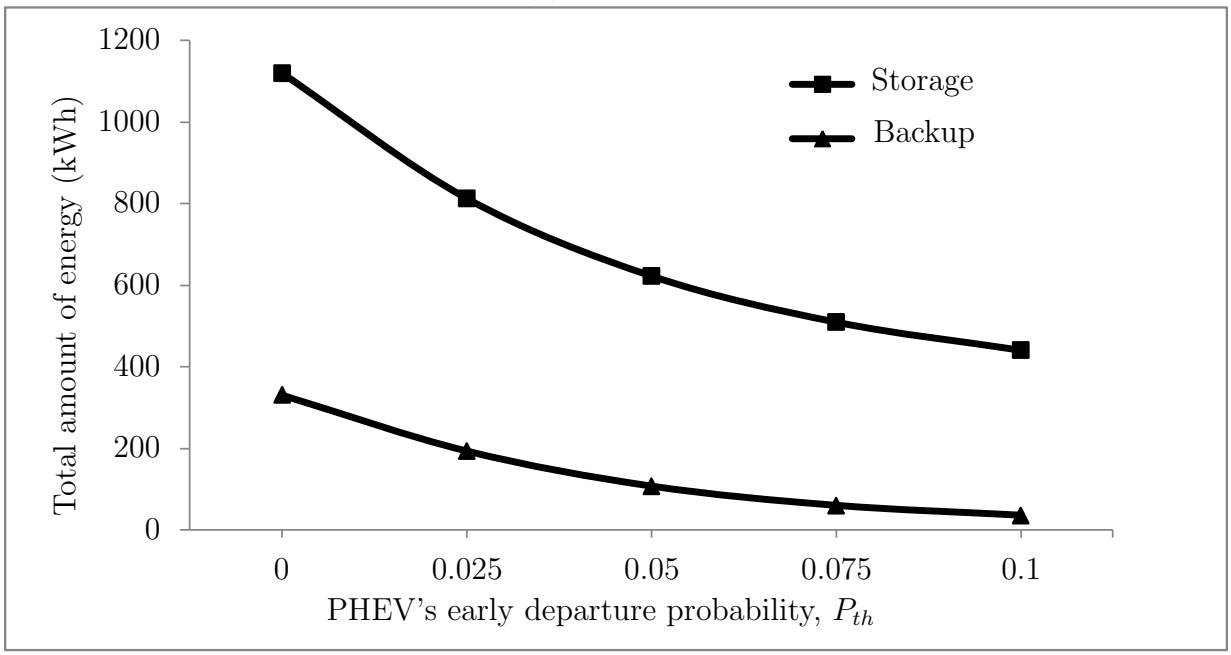

(b) $\alpha_{soc} = 0.5$.

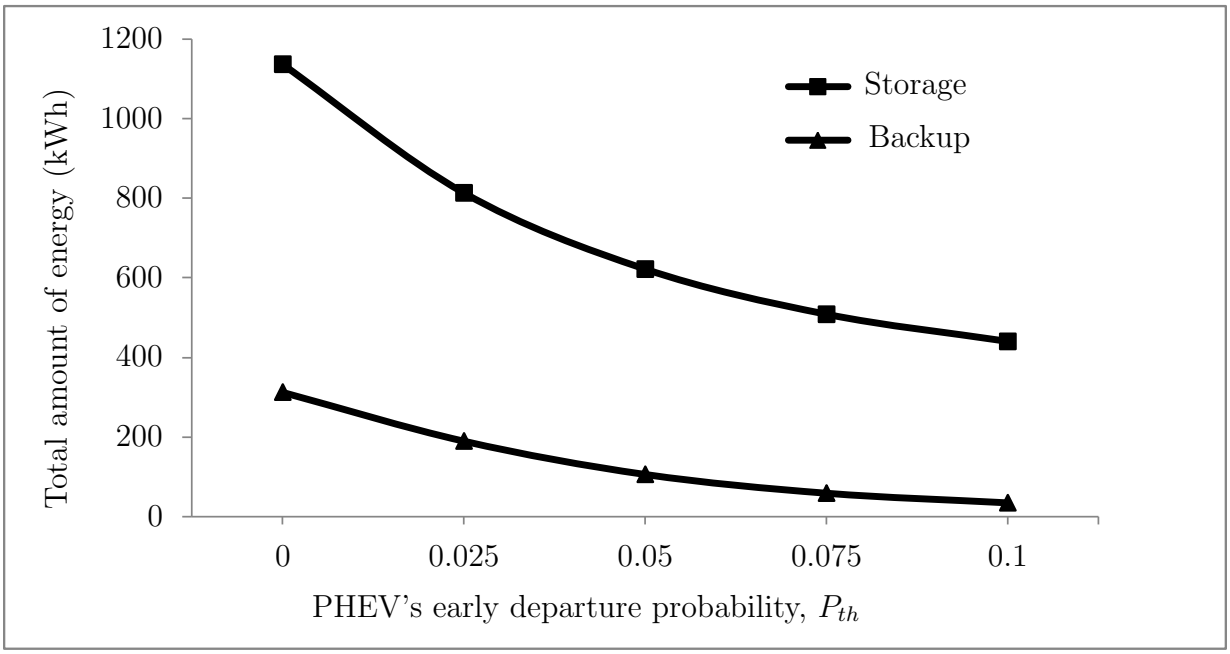

(c) $\alpha_{soc} = 0.9$.

Figure 4.8: Total amount of storage and backup energy.

namely ratio of RES supply over total supply, total amount of storage energy (γ_S), and total amount of backup energy decrease gradually with an increasing value of P_{th}.

4.6 Summary

In summary, the impact of α_{soc} variations is only limited to the performance metrics of the total energy from V2V charging and total extra energy conversion loss due to V2V operation. Moreover, such impact seizes to exist when the PHEVs start to depart early from the parking lot. It is also observed that early departures of PHEVs are not desirable as they have a reverse impact on all the performance metrics. It is also observed that the total amount of energy transaction in the V2V operations never exceed the total amount

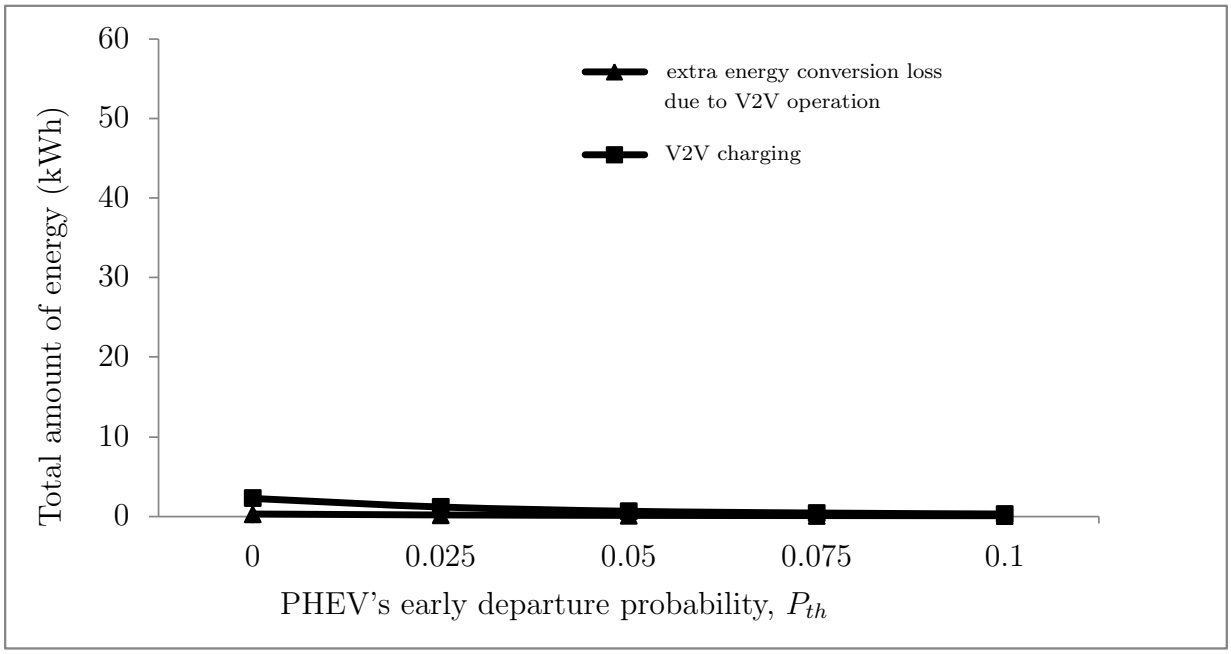

(a) For $\alpha_{soc} = 0.1$.

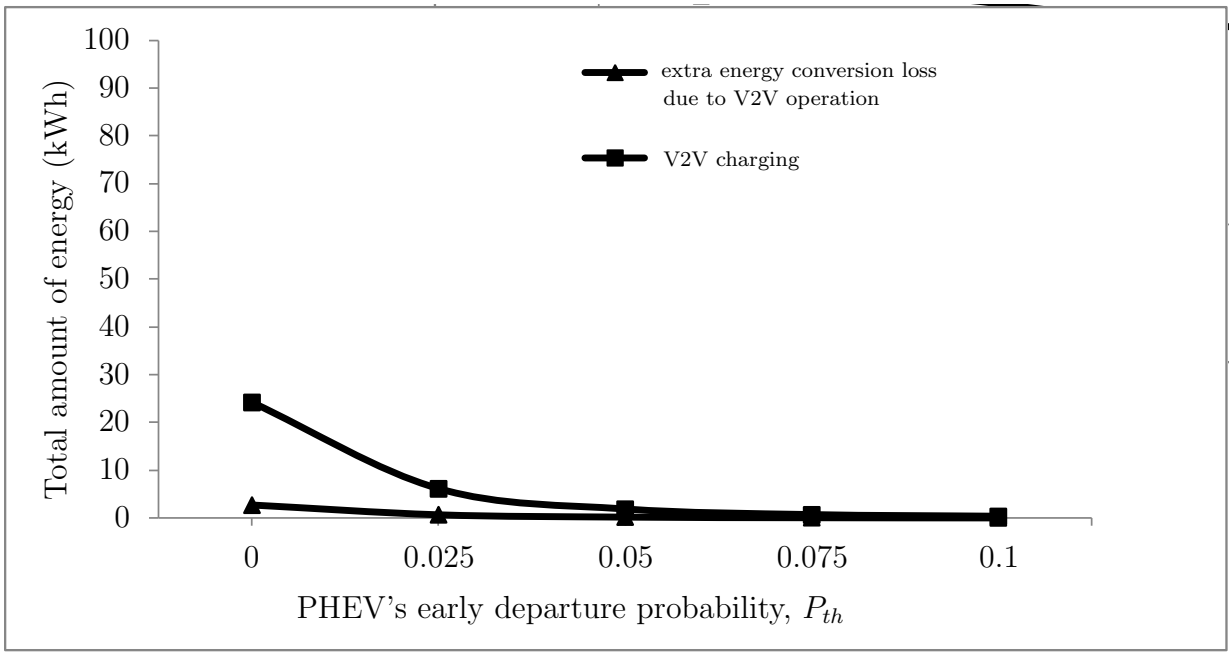

(b) For $\alpha_{soc} = 0.5$.

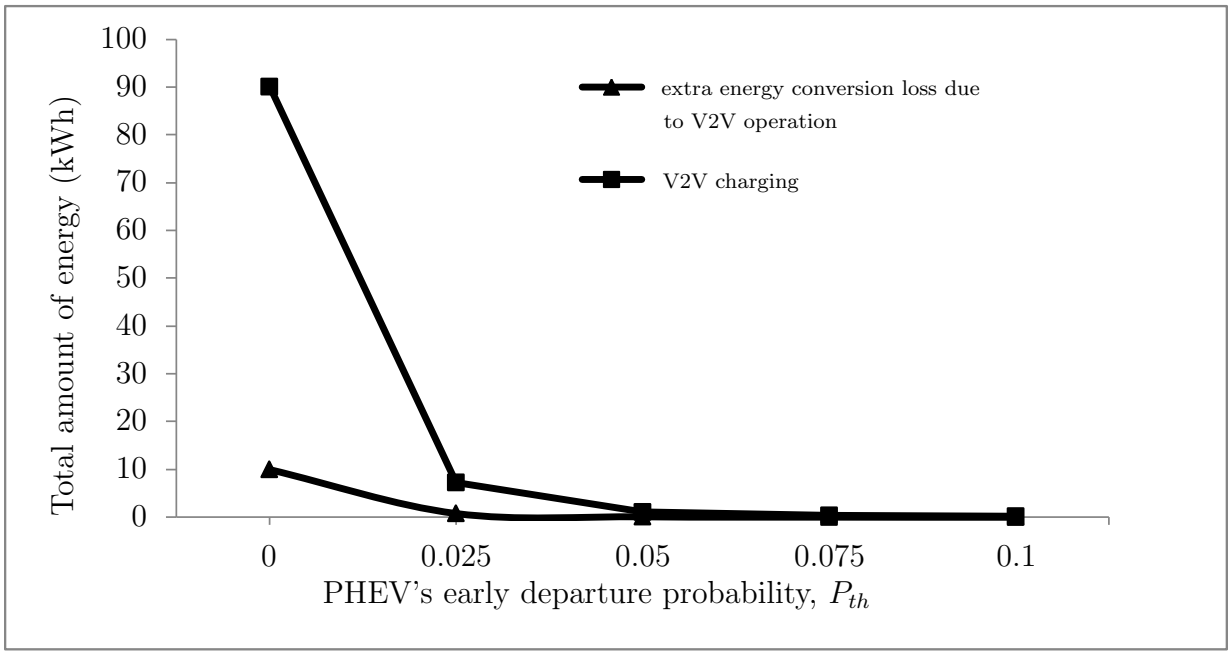

(c) For $\alpha_{soc} = 0.9$.

Figure 4.9: Total energy from V2V charging and Total extra energy conversion loss due to V2V operation.

of energy delivered by the surplus RES supply for the given RES profile. This shows that the V2V operation is effective for the given RES profile.

Chapter 5

Conclusion and Future Work

The performance of vehicle-to-vehicle operation depends upon how the total number of vehicles are divided into two groups, namely a charging group and a discharging group. An algorithm should aim at optimally dividing the total number of vehicles into the two groups such that the energy transaction in the V2V operation is maximized. The algorithm must satisfy the constraints imposed by vehicle owners such that as a minimum SOC of the vehicle battery is maintained before it departs for its next trip.

The decision rule to determine if a given vehicle should discharge in the V2V operation should governed mainly by three factors: i) SOC of vehicle battery, ii) remaining time before vehicle departs, and iii) likelihood of surplus RES in the future. In this research, we have addressed first two factors only to limit the scope of the research.

We can summarize our research contributions as

- We proposed a novel vehicle-to-vehicle power transfer operation towards enhancing renewable energy sources utilization in the microgrid. To the best of our knowledge,

the idea of vehicle-to-vehicle operation is a novel approach. The main idea of the V2V operation is to enhance the storage capacity of V2G system in the future. The V2V operation transfer the energy from source vehicles (which stay parked for relatively longer time) to destination vehicles (which are going to depart soon). In this way, the source vehicles are ready to accept more energy in the future. Finally, the renewable energy sources will be better utilized for the given condition that there will be a sufficient amount of surplus RES generation in the future.

- We have presented a comprehensive analysis of impacts of SOC and mobility pattern of vehicles on the overall performance. It was found that the SOC of vehicle battery should be given more priority over the remaining time before the vehicle departs. Similarly, it was found that when vehicles start to depart unexpectedly the performance starts degrading rapidly.

5.1 Future Work

In this research, we focused on studying the impacts of SOC and mobility pattern of vehicles on the V2V operation performance. As mentioned earlier, the impact of likelihood of surplus RES in the future should also be analyzed. If there is a very low chance of surplus RES in the future, the V2V operation will become meaningless because the only motivation is to utilize the future surplus RES. By incorporating the prediction of future surplus RES while making a decision whether or not a V2V operation is invoked, the overall algorithm should become more meaningful. Moreover, we have chosen a fixed value of V2V threshold, Ω. Hence, the impact of Ω on the V2V performance should also be analyzed in

the future work.

Appendices

Appendix A

Algorithms

A.1 Main Algorithm

1: **set** I, N

2: **for** $n \leftarrow 1$ to N **do**

3: generate $R[n]$ and $p_i[n], \forall i \in \{1, 2, 3, ..., I\}$

4: compute $L_N[n] = L[n] - R[n]$, and $\tau_i[n], \forall i \in \{1, 2, 3, ..., I\}$

5: **if** $L_N[n] \geq 0$ **then**

6: run **Backup Algorithm** (Section A.3)

7: **end if**

8: **if** $L_N[n] < 0$ **then**

9: go to **Storage Algorithm Block** (Section A.2)

10: **end if**

11: compute $G[n], R_c[n], G_L[n], G[n]$

12: limit $C^{agg}[n]$ and $D^{agg}[n]$ to limiting values C^{agg}_{max} and D^{agg}_{max} respectively

13: compute $G[n], R_c[n], G_L[n], L_c[n]$

14: **end for**

A.2 Storage Algorithm Block

1: **for** $i \leftarrow N$ **do**

2: compute the minimum demand of PHEV i, $\delta_{i,min}[n]$

$$\delta_{i,min}[n] = \begin{cases} 0, & n \notin M_i \text{ or } \tau_i[n] = 0 \\ \dfrac{e - \beta\overline{x_i}}{\tau_i[a_i]}, & n = a_i \\ \dfrac{e - \beta \cdot x_i[n-1]}{\tau_i[n]}, & \text{otherwise} \end{cases}$$

3: **end for**

4: compute total amount of minimum PHEV demand,

$$sum_\delta = \sum_{i=1}^{I} \delta_{i,min}[n]$$

5: **if** $sum_\delta > |L_N[n]|$ *(i.e., Necessary condition for a V2V operation)* **then** run Algorithm A.4: **V2V Algorithm**

6: **else**

7: Begin **Typical Storage Algorithm** as follows

8: **for** $i \leftarrow N$ **do**

9: compute

$$c_{V2G,i}[n] = \frac{\delta_{i,min}[n]}{sum_\delta}|L_N[n]|$$

10: **if** $c_{V2G,i}[n] > \min(C^{max}, e - x_i[n-1])$ **then**

11: $c_{V2G,i}[n] = \min(C^{max}, e - x_i[n-1])$ and divide the remaining energy to other PHEVs

12: **end if**

13: **end for**

14: **if** $|L_N[n]| > \sum_{i=1}^{I} c_{V2G,i}[n]$ **then** $R_c[n] = L_N[n] - \sum_{i=1}^{I} c_{V2G,i}[n]$

15: **end if**

16: **if** $\delta_{i,min}[n] > c_{V2G,i}[n]$ **then** $c_{G,i}[n] = \delta_{i,min}[n] - c_{V2G,i}[n]$

17: **end if**

18: **end if**

A.3 Backup Algorithm

1: **for** $i \leftarrow 1$ to I **do**

2: compute maximum discharge rate of PHEV i,

$$\delta_{i,max}[n] = \begin{cases} 0, & n = 1 \text{ or } n = a_i \\ \dfrac{x_i[n-1] - \overline{x_i}}{\tau_i[n]}, & \text{otherwise.} \end{cases}$$

3: **if** $\delta_{i,max}[n] \leq 0$ **then** $\delta_{i,max} = 0$ and $c_{G,i}[n] = \min(C^{max}, e - x_i[n-1])$

4: **else** $c_{G,i}[n] = 0$

5: **end if**

6: **end for**

7: **if** $\sum_{i=1}^{I} \delta_{i,max}[n] \geq L_N[n]$ **then**

$$d_{V2G,i}[n] = \frac{\delta_{i,max}[n]}{\sum_{i=1}^{I} \delta_{i,max}[n]} L_N[n], \forall i \in \{1, 2, ..., I\},$$

8: and $G_L[n] = 0$

9: **else** set $d_{V2G,i}[n] = \delta_{i,max}[n], \forall i \in \{1, 2, ..., I\}$,

10: and $G_L[n] = L_N[n] - \sum_{i=1}^{I} \delta_{i,max}[n]$

11: **end if**

12: **if** $G_L[n] > G^{max}$ **then** $L_c[n] = G_L[n] - G^{max}$

13: **else** $L_c[n] = 0$

14: **end if**

15: **for** $i \leftarrow 1$ to I **do**

16: compute $c_i[n] = c_{V2G,i}[n] + c_{v,i}[n] + c_{G,i}[n]$ and $d_i[n] = d_{V2G,i}[n] + d_{v,i}[n]$

17: update $x_i[n] = \beta x_i[n-1] + c_i[n]\eta_c - \frac{d_i[n]}{\eta_d}$

18: **end for**

A.4 V2V Algorithm

1: **for** $i \leftarrow 1$ to I **do**

2: compute metric $\omega_i[n]$

3: **if** $\omega_i[n] \geq \Omega$ **then** *(from research question 1)*, assign PHEV i to set $\Psi_{d,n}$, and compute $\overline{d_{v,i}[n]}$ *(from research question 2)*

4: **else** assign PHEV i to set $\Psi_{c,n}$, and $\overline{d_{v,i}[n]} = 0$

5: **end if**

6: **end for**

7: compute

$$\text{total mimumum demand, } sum_{cv,n} = \sum_{i \in \Psi_{c,n}} \delta_{i,min}[n],$$

$$\text{total maximum supply, } sum_{dv,n} = \sum_{i \in \Psi_{d,n}} \overline{\delta_{v,i}[n]}$$

8: **if** ($sum_{cv,n} > |L_N[n]|$ and $\Psi_{d,n} \neq \emptyset$), *the sufficient condition for a V2V operation,* **then**

9: compute

$$c_{V2G,i}[n] = \frac{\delta_{i,min}}{sum_{cv,n}} |L_N[n]|, \qquad \forall i \in \Psi_{c,n}$$

and limit $c_{V2G,i}[n]$ to limiting values C^{max} and $(e - x_i[n-1])$

10: compute

$\Delta_R = sum_{cv,n} - |L_N[n]|$

11: **if** $\Delta_R > sum_{dv,n}$ **then**

12: $d_{v,i}[n] = \overline{d_{v,i}[n]}$ and $c_{G,i}[n] = 0, \forall i \in \Psi_{d,n}$;

13: $c_{v,i}[n] = \frac{\delta_{i,min}}{sum_{cv,n}} sum_{dv,n}, \forall i \in \Psi_{c,n}$;

14: **else**

15: $d_{v,i}[n] = \frac{\overline{d_{v,i}[n]}}{sum_{dv,n}} \Delta_R$ and $c_{G,i}[n] = 0; \forall i \in \Psi_{d,n}$

16: $c_{v,i}[n] = \delta_{i,min}[n] - c_{V2G,i}[n]; \forall i \in \Psi_{c,n}$

17: **end if**

18: **for all** $i \in \Psi_{c,n}$ **do**

19: limit $c_{v,i}[n]$ to limiting values $(C^{max} - c_{V2G,i}[n])$ and $(e - x_i[n-1] - c_{V2G,i}[n])$

20: compute $c_{G,i}[n] = \delta_{i,min}[n] - c_{V2G,i}[n] - c_{v,i}[n], \forall i \in \Psi_{c,n}$,

21: limit $c_{G,i}[n]$ to limiting values $(C^{max} - c_{V2G,i}[n] - c_{v,i}[n])$ and $(e - x_i[n-1] - c_{V2G,i}[n] - c_{v,i}[n])$

22: **end for**

23: **if** $\sum_{i=1}^{I} d_{v,i}[n] > \sum_{i=1}^{I} c_{v,i}[n]$ **then**

24: reset $d_{v,i}[n] = d_{v,i}[n] - \{\frac{\overline{d_{v,i}[n]}}{sum_{dv,n}} \cdot (\sum_{i=1}^{I} d_{v,i}[n] - \sum_{i=1}^{I} c_{v,i}[n])\}, \forall i \in \Psi_{d,n}$

25: **end if**

26: **else** goto step 7 of **Storage Algorithm Block** (Section A.2) i.e., **Typical Storage Algorithm**

27: **end if**

Bibliography

[1] Willett Kempton and Jasna Tomić. Vehicle-to-grid power implementation: From stabilizing the grid to supporting large-scale renewable energy. *Journal of Power Sources*, 144(1):280–294, 2005.

[2] Robert H Lasseter. Microgrids. In *Power Engineering Society Winter Meeting, 2002. IEEE*, volume 1, pages 305–308. IEEE, 2002.

[3] S. Bahramirad and H. Daneshi. Optimal sizing of smart grid storage management system in a microgrid. In *Innovative Smart Grid Technologies (ISGT), 2012 IEEE PES*, pages 1–7, Jan 2012.

[4] Stephen McCluer and Jean-Francois Christin. Comparing data center batteries, flywheels, and ultracapacitors. *White Paper*, 65, 2008.

[5] M.H. Ahmed, K. Bhattacharya, and M.M.A. Salama. Probabilistic distribution load flow with different wind turbine models. *Power Systems, IEEE Transactions on*, 28(2):1540–1549, May 2013.

[6] Robert H Lasseter and Paolo Paigi. Microgrid: a conceptual solution. In *Power Electronics Specialists Conference, 2004. PESC 04. 2004 IEEE 35th Annual*, volume 6, pages 4285–4290. IEEE, 2004.

[7] A Zahedi. Maximizing solar pv energy penetration using energy storage technology. *Renewable and Sustainable Energy Reviews*, 15(1):866–870, 2011.

[8] Shaghayegh Bahramirad, Wanda Reder, and Amin Khodaei. Reliability-constrained optimal sizing of energy storage system in a microgrid. *Smart Grid, IEEE Transactions on*, 3(4):2056–2062, 2012.

[9] Willett Kempton and Jasna Tomić. Vehicle-to-grid power fundamentals: calculating capacity and net revenue. *Journal of Power Sources*, 144(1):268–279, 2005.

[10] Ting Wu, Qiang Yang, Zhejing Bao, and Wenjun Yan. Coordinated energy dispatching in microgrid with wind power generation and plug-in electric vehicles. *Smart Grid, IEEE Transactions on*, 4(3):1453–1463, Sept 2013.

[11] C Battistelli, L Baringo, and AJ Conejo. Optimal energy management of small electric energy systems including v2g facilities and renewable energy sources. *Electric Power Systems Research*, 92:50–59, 2012.

[12] Sheikh Mominul Islam. Increasing wind energy penetration level using pumped hydro storage in island micro-grid system. *International Journal of Energy and Environmental Engineering*, 3(1):1–12, 2012.

[13] N Hamsic, A Schmelter, A Mohd, E Ortjohann, E Schultze, A Tuckey, and J Zimmermann. Increasing renewable energy penetration in isolated grids using a flywheel

energy storage system. In *Power Engineering, Energy and Electrical Drives, 2007. POWERENG 2007. International Conference on*, pages 195–200. IEEE, 2007.

[14] Yu Zhang, N. Gatsis, and G.B. Giannakis. Robust energy management for microgrids with high-penetration renewables. *Sustainable Energy, IEEE Transactions on*, 4(4):944–953, Oct 2013.

[15] M. Ross, R. Hidalgo, C. Abbey, and G. Joos. Analysis of energy storage sizing and technologies. In *Electric Power and Energy Conference (EPEC), 2010 IEEE*, pages 1–6, Aug 2010.

[16] H. Farhangi. The path of the smart grid. *Power and Energy Magazine, IEEE*, 8(1):18–28, January 2010.

[17] T. Ackermann and V. Knyazkin. Interaction between distributed generation and the distribution network: operation aspects. In *Transmission and Distribution Conference and Exhibition 2002: Asia Pacific. IEEE/PES*, volume 2, pages 1357–1362 vol.2, Oct 2002.

[18] Robert Lasseter, Abbas Akhil, Chris Marnay, John Stephens, Jeff Dagle, Ross Guttromson, A Sakis Meliopoulous, Robert Yinger, and Joe Eto. Integration of distributed energy resources. the certs microgrid concept. 2002.

[19] Omar Hafez and Kankar Bhattacharya. Optimal planning and design of a renewable energy based supply system for microgrids. *Renewable Energy*, 45:7–15, 2012.

[20] H.S.V.S.K. Nunna and S. Ashok. Optimal management of microgrids. In *Innovative Technologies for an Efficient and Reliable Electricity Supply (CITRES), 2010 IEEE Conference on*, pages 448–453, Sept 2010.

[21] A. Hooshmand, M.H. Poursaeidi, J. Mohammadpour, H.A. Malki, and K. Grigoriads. Stochastic model predictive control method for microgrid management. In *Innovative Smart Grid Technologies (ISGT), 2012 IEEE PES*, pages 1–7, Jan 2012.

[22] Xiaohong Guan, Zhanbo Xu, and Qing-Shan Jia. Energy-efficient buildings facilitated by microgrid. *Smart Grid, IEEE Transactions on*, 1(3):243–252, Dec 2010.

[23] M.E. Khodayar, M. Barati, and M. Shahidehpour. Integration of high reliability distribution system in microgrid operation. *Smart Grid, IEEE Transactions on*, 3(4):1997–2006, Dec 2012.

[24] N. Saito, T. Niimura, K. Koyanagi, and R. Yokoyama. Trade-off analysis of autonomous microgrid sizing with pv, diesel, and battery storage. In *Power Energy Society General Meeting, 2009. PES '09. IEEE*, pages 1–6, July 2009.

[25] Wencong Su, H. Eichi, Wente Zeng, and Mo-Yuen Chow. A survey on the electrification of transportation in a smart grid environment. *Industrial Informatics, IEEE Transactions on*, 8(1):1–10, Feb 2012.

[26] E. Sortomme and M.A. El-Sharkawi. Optimal charging strategies for unidirectional vehicle-to-grid. *Smart Grid, IEEE Transactions on*, 2(1):131–138, March 2011.

[27] Hao Liang, Bong Jun Choi, Weihua Zhuang, and Xuemin Shen. Optimizing the energy delivery via v2g systems based on stochastic inventory theory. *Smart Grid, IEEE Transactions on*, 4(4):2230–2243, Dec 2013.

[28] Hao Liang, Bong Jun Choi, Weihua Zhuang, and Xuemin Shen. Towards optimal energy store-carry-and-deliver for phevs via v2g system. In *INFOCOM, 2012 Proceedings IEEE*, pages 1674–1682, March 2012.

[29] Yifeng He, B. Venkatesh, and Ling Guan. Optimal scheduling for charging and discharging of electric vehicles. *Smart Grid, IEEE Transactions on*, 3(3):1095–1105, Sept 2012.

[30] E. Sortomme and M.A. El-Sharkawi. Optimal scheduling of vehicle-to-grid energy and ancillary services. *Smart Grid, IEEE Transactions on*, 3(1):351–359, March 2012.

[31] U.C. Chukwu and S.M. Mahajan. V2g electric power capacity estimation and ancillary service market evaluation. In *Power and Energy Society General Meeting, 2011 IEEE*, pages 1–8, July 2011.

[32] Yuchao Ma, T. Houghton, A. Cruden, and D. Infield. Modeling the benefits of vehicle-to-grid technology to a power system. *Power Systems, IEEE Transactions on*, 27(2):1012–1020, May 2012.

[33] Scott B Peterson, JF Whitacre, and Jay Apt. The economics of using plug-in hybrid electric vehicle battery packs for grid storage. *Journal of Power Sources*, 195(8):2377–2384, 2010.

[34] C. Hutson, G.K. Venayagamoorthy, and K.A. Corzine. Intelligent scheduling of hybrid and electric vehicle storage capacity in a parking lot for profit maximization in grid power transactions. In *Energy 2030 Conference, 2008. ENERGY 2008. IEEE*, pages 1–8, Nov 2008.

[35] Sekyung Han, Soohee Han, and K. Sezaki. Development of an optimal vehicle-to-grid aggregator for frequency regulation. *Smart Grid, IEEE Transactions on*, 1(1):65–72, June 2010.

[36] T. Markel, M. Kuss, and P. Denholm. Communication and control of electric drive vehicles supporting renewables. In *Vehicle Power and Propulsion Conference, 2009. VPPC '09. IEEE*, pages 27–34, Sept 2009.

[37] S. Grillo, M. Marinelli, S. Massucco, and F. Silvestro. Optimal management strategy of a battery-based storage system to improve renewable energy integration in distribution networks. *Smart Grid, IEEE Transactions on*, 3(2):950–958, June 2012.

[38] Cui Shumei, Liu Xiaofei, Tian Dewen, Zhang Qianfan, and Song Liwei. The construction and simulation of v2g system in micro-grid. In *Electrical Machines and Systems (ICEMS), 2011 International Conference on*, pages 1–4. IEEE, 2011.

[39] Robert H Lasseter. Microgrids. In *Power Engineering Society Winter Meeting, 2002. IEEE*, volume 1, pages 305–308. IEEE, 2002.

[40] Rui Huang, S.H. Low, Ufuk Topcu, K.M. Chandy, and C.R. Clarke. Optimal design of hybrid energy system with pv/wind turbine/storage: A case study. In *Smart Grid*

Communications (SmartGridComm), 2011 IEEE International Conference on, pages 511–516, Oct 2011.

[41] Seung-Tea Cha, Dong-Hoon Jeon, In-Su Bae, Il-Ryong Lee, and Jin-O Kim. Reliability evaluation of distribution system connected photovoltaic generation considering weather effects. In *Probabilistic Methods Applied to Power Systems, 2004 International Conference on*, pages 451–456. IEEE, 2004.

[42] Liang Huishi, Su Jian, and Liu Sige. Reliability evaluation of distribution system containing microgrid. In *Electricity Distribution (CICED), 2010 China International Conference on*, pages 1–7. IEEE, 2010.

[43] Daniel Weisser. A wind energy analysis of grenada: an estimation using the weibulldensity function. *Renewable Energy*, 28(11):1803–1812, 2003.

[44] Amotz Bar-Noy, Yi Feng, Matthew P Johnson, and Ou Liu. When to reap and when to sow–lowering peak usage with realistic batteries. In *Experimental Algorithms*, pages 194–207. Springer, 2008.

[45] Rahul Urgaonkar, Bhuvan Urgaonkar, Michael J Neely, and Anand Sivasubramaniam. Optimal power cost management using stored energy in data centers. In *Proceedings of the ACM SIGMETRICS joint international conference on Measurement and modeling of computer systems*, pages 221–232. ACM, 2011.

[46] Battery and energy technologies: Battery performance characteristic. [Online], Website. `http://mpoweruk.com/performance.htm`.

[47] P. Richardson, D. Flynn, and A. Keane. Local versus centralized charging strategies for electric vehicles in low voltage distribution systems. *Smart Grid, IEEE Transactions on*, 3(2):1020–1028, June 2012.